REMARKS

Claims 1-10 and 12-15 are pending in the present application. Claims 12-15 are withdrawn from consideration, and claims 1-10 are currently rejected.

Rejection under 35 U.S.C. 112, second paragraph

The Examiner rejects the claims as unclear because it is allegedly not clear whether Applicants are claiming the preparation of acrylic acid or acrylonitrile or a combination of the two. Applicants herein amend claim 1 to define a catalyst for an oxidation reaction of a hydrocarbon which can be an alkane, an alkene or mixtures thereof. Furthermore, the catalyst is defined by its chemical nature and X-ray diffraction lines, and using the same in preparing acryclic acid of acrylonitrile does not depend upon the catalyst, but on other reaction conditions, such as the starting product and other reagents employed. If one adds ammonia one obtains acrylonitrile, but if one employs oxygen one obtains acrylic acid in the reaction with propane. Therefore, the nature of the catalyst is completely independent of the process in which it is used. Applicants submit that claim 1 as presently amended clarifies that the catalyst is intended for use in an oxidation reaction of concrete type of hydrocarbons.

The Examiner also indicates that the parameters h, i, j, k and x do not have antecedent basis because they do not appear in claim 1. Applicants herein include the empirical formula in amended claim 1, but without limiting the values of the parameters. Applicants submit that since information is included regarding the four essential elements (Mo, Te, V and Cu), the concrete additional elements (A) that can be present, the fact that Mo, V, Te and Cu are present in the form of at least and oxide, the proportion of Mo related to the proportion of the remainder of the elements in the catalyst, and the presence of concrete five X-ray diffraction lines, the catalysts are clearly defined so as to reasonably apprise one of ordinary skill in the art of the metes and bounds of the invention. Further, Applicants respectfully submit that further defining the values of h, i, and j considering that the value of x clearly depends on the values of the other three mentioned parameters, would unnecessarily limit the scope of the claims.

Rejection under 35 U.S.C. 103

The Examiner rejects all of the claims as allegedly obvious over Takahashi *et al.*, U.S. Patent 5,994,580. The Examiner admits that Takahashi *et al.* do not teach the particular x-ray diffraction angles of the catalyst, however, the Examiner says that these represent no more than manipulation of parameters to improve yield and/or selectivity.

Applicants respectfully disagree. The fact that the process can be coincident, a reaction of propane oxidation, does not mean that the catalysts are the same. Takahashi *et al.* teach catalysts including Mo, V, Sb and A. Moreover, Takahashi *et al.* teach that A can be one or more of Nb, Ta, Sn, W, Ti, Ni, Fe, Cr and Co. Therefore, it is clear that Te is never present in the catalysts of Takahashi whereas Te is an essential element in the catalysts of the present invention. Furthermore, the catalysts of Takahashi *et al.* all contain Sb whereas antimony is not a part of the catalysts of the present invention. Still further, the catalysts of the present invention all contain Cu whereas the catalysts of Takahashi *et al.* never contain copper. In short, the differences between Takahashi *et al.* and the present invention are not simply the presence or absence of a single element, but in that the coincident elements necessary are only two considering that the catalysts of Takahashi *et al.* as well as those of the present invention have in all cases at least four different elements.

Applicants wish to clarify that the X-ray diffraction pattern is one of the clearest forms of identifying a chemical compound, and the five lines included in claim 1 are intense lines and are provided with an error in the diffraction angle of ±4. Therefore, Applicants submit that it is not entirely true that the X-ray data given may have been manipulated. In view of the foregoing, it is clear that Takahashi *et al.* do not teach or suggest the catalysts of the present invention.

Still further demonstrating the patentability of the present invention, Applicants submit that Takahashi *et al.* obtain the best results with catalysts containing added elements such as K. Additionally, catalysts containing Sb, such as those of Takahashi *et al.* also require potassium in order to obtain higher selectivity to acrylic acid, whereas the

element copper in a catalyst such as Mo-V-Te-Nb demonstrates very different behavior. To clarify this, Applicants respectfully direct the Examiner's attention to Blasco *et al.*, *Journal of Catalysis* 228, 362 (2004), a copy of which is submitted herewith, wherein it is shown that an Sb containing catalyst also necessarily requires potassium in order to lower the catalyst acidity. It has been observed that in a Mo-V-Sb-O catalyst, the number of acid centers decreases with the amount of the potassium content, demonstrating that the best results are obtained with a certain K amount. Hence, the catalysts of Takahashi *et al.* demonstrate better results when they contain potassium.

In contrast to the foregoing, in a catalyst having tellurium, such as those of the present invention, the number and strength of the acid centers is much lower than the number and strength of the acid centers in a catalyst having Sb. This fact is clearly demonstrated in by Concepción *et al.*, *Applied Catalysis* A: General 278, 45 (2004), a copy of which is submitted herewith. Concepción *et al.* also demonstrate that the effect of the potassium element in the catalysts of Takahashi *et al.* is not related to the effect of the presence of copper in the catalysts of the instant invention.

Applicants submit as well a copy of Baca *et al.*, *Catalysis Communications*, 6, 215 (2005) to further demonstrate the differences in the acid centers of the catalysts. In view of the foregoing explanations, the catalysts of Takahashi *et al.* and those of the instant invention are quite different, and the differences are obviously reflected in their different mechanisms of action.

It is a fundamental principle of the patent law that secondary considerations may be used to rebut a prima facie case of obviousness. One such secondary consideration is unexpectedly superior results or properties. In the instant case, *assuming arguendo*, that a proper *prima facie* case of obviousness could be said to exist, secondary considerations still establish patentability. An advantage of the present invention catalysts over those of Takahashi *et al.* is avoiding undesirable side effects. Antimony is highly toxic, causing in small doses headache, dizziness and depression, and in larger doses death in a few days. In contrast, tellurium is considered to be mildly toxic and acute poisoning with Te is rare.

This advantage alone establishes the patentability of the present invention over Takahashi *et al.*

CONCLUSION

Entry of the foregoing amendments and remarks into the record of the above identified application is respectfully requested. Applicants submit that the claims are now all in condition for allowance and early notification of such is solicited. If any issues may be resolved telephonically, the Examiner is invited to contact the undersigned at the telephone number indicated below.

Respectfully submitted,

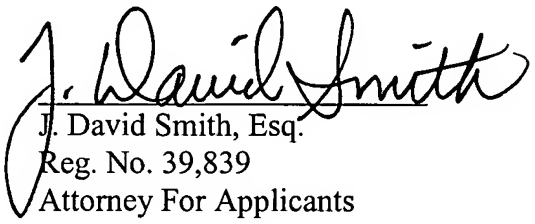

J. David Smith, Esq.
Reg. No. 39,839
Attorney For Applicants

KLAUBER & JACKSON
411 Hackensack Avenue
Hackensack, New Jersey 07601
(201) 487-5800

Available online at www.sciencedirect.com
SCIENCE DIRECT®
Catalysis Communications 6 (2005) 215–220
CATALYSIS COMMUNICATIONS
www.elsevier.com/locate/catcom

Fourier transform infrared spectroscopic study of surface acidity by pyridine adsorption on the *M1* active phase of the MoVTe(Sb)NbO catalysts used in propane oxidation

M. Baca [a,1], A. Pigamo [a,b], J.L. Dubois [b], J.M.M. Millet [a,*]

[a] *Institut de Recherches sur la Catalyse, CNRS, Conventionné avec l'Université Claude Bernard, Lyon I, 2 Avenue A. Einstein, F-69626 Villeurbanne Cedex, France*
[b] *Atofina S.A. Centre de Recherches Rhône-Alpes, Lyon, France*

Received 11 October 2004; accepted 22 December 2004
Available online 25 January 2005

Abstract

The adsorption of pyridine on the surface of the *M1* active phase of the MoVTe(Sb)O catalysts has been studied for the determination of the Brønsted and Lewis acid sites. The results obtained showed medium Lewis and Brønsted acidity for antimony containing phases and low Lewis and Brønsted acidity for tellurium ones. The incorporation of niobium in the *M1* phases resulted in a decrease of both acidities. The samples characterized have been tested as catalysts in the oxidation of propane to acrylic acid. The results obtained allowed to propose correlations between the acidic properties and the catalytic selectivity.

Keywords: Oxidation of propane; Acrylic acid; MoVTe(Sb)NbO catalysts; Pyridine adsorption

1. Introduction

The direct oxidation of propane to acrylic acid has attracted a lot of attention in the past decade. Progress has been made with the discovery of new active and selective oxide based catalysts [1,2]. These catalysts, first patented for propane ammoxidation to acrylonitrile, contain four metallic elements: Mo, V, Te or Sb and Nb. Each four element is contained into two phases, named *M1* and *M2*, which are solid solutions [3–6]. The phase *M1* has been demonstrated to be the active and selective phase for propane oxidation or ammoxidation and responsible of the performance for the catalysts [3,7]. It crystallizes in the orthorhombic system and can contain either Te or Sb cations with a formula that has been reported as $(AO)_{2-2x}(A_2O)_xM_{20}O_{56}$ with A = Sb or Te, M = Mo, V, Nb and $0 \leqslant x \leqslant 1$ [6,8]. The V/Mo and Nb/Mo ratios can vary, but are generally close to 0.3 and 0.1. The structure model for the *M1* phases, initially proposed based on an isomorphism with the phase $Cs_{0.7}(Nb,W)_5O_{14}$ [5], has been ascertained and the atomic positions and occupancies have been determined [9,10]. The structure can be described by a corner sharing MO_6 (M = Mo, V, Nb) octahedra network with tellurium or antimony cations and oxygen anions occupying sites in hexagonal channels formed by the octahedra. Besides hexagonal channels, pentagonal and heptagonal channels are present and oriented in the same direction. The heptagonal channels have been reported to be empty and the pentagonal ones occupied by Nb cations. Vanadium and molybdenum are not equally distributed in the octahedral network but occupy preferentially certain sites.

* Corresponding author. Tel.: +33 0 472445317; fax: +33 0 472445399.
E-mail address: millet@catalyse.cnrs.fr (J.M.M. Millet).
[1] Member of the European CONCORDE Coordination Action.

1566-7367/$ - see front matter © 2005 Elsevier B.V. All rights reserved.
doi:10.1016/j.catcom.2004.12.010

Previous studies by Ueda and Oshihara [11] have shown that the crystalline *M1* phases, with Te or Sb, could be obtained without niobium. These studies ruled out the hypothesis formulated earlier on the role of niobium in stabilizing the structure [12,13] and it is still not fully understood why its presence increases the selectivity to acrylic acid by about 15–20%. The last studies conducted on this subject proposed that niobium changes the catalyst morphology or suppress further oxidation of acrylic acid in CO_x [14].

It has been widely demonstrated that acidity may have a relevent role on the oxidation or on the oxidative dehydrogenation activity and selectivity of a catalyst. The aim of the present study is to determine the types of acid sites present in *M1* phases with different compositions by taking FT-IR spectra from their surface during the adsorption of pyridine. Adsorption of a base like pyridine is commonly use for the determination of acidity of solid surfaces with the formation of pyridinium ions with Brønsted centers and coordination of pyridine on Lewis ones. Four *M1* phases have been studied, two containing Sb with and without Nb: (*M1* (Sb)) and *M1*(Sb–Nb) and two containing Te with and without Nb: (*M1*(Te)) and *M1*(Te–Nb). They allowed to determine the effect of the presence of the cited cations on the acidity of the phase. Catalytic properties of the studied phases have been determined for the oxidation of propane to acrylic acid and correlations have been searched between the acidity and the catalytic properties.

2. Experimental

The preparation of the *M1*(Te–Nb) and *M1*(Sb–Nb) phases took place in two steps. In a first step, a *M1* and *M2* phase mixture was prepared according to patented methods from an aqueous slurry comprising Mo, V, Te(Sb) and Nb precursors in the ratio Mo/V/Te(Sb)/Nb = 1/0.33/0.22(0.15)/0.11 [15,16]. The slurries were evaporated to dryness at 383 K and successively calcined at 573 K under air and at 873 K under nitrogen for 2 h. In a second step, the biphasic catalyst was stirred in a 15% hydrogen peroxide aqueous solution at room temperature for 2 h. Under such conditions the *M2* phase was completely dissolved. The solids recovered were washed with water, dried at 383 K and calcined under nitrogen at 873 K for 2 h.

Pure *M1*(Te) and *M1*(Sb) were prepared by hydrothermal synthesis according to a procedure described elsewhere [11]. For *M1*(Te), to 20 mL of water were successively added 5.35 g of ammonium heptamolybdate and 0.80 g of tellurium dioxide. Separately, an aqueous solution of vanadium was prepared by dissolving 3.94 g of hydrated vanadyl sulfate in 10 mL of water. Both solutions were mixed at room temperature and stirred for 10 min before being introduced into the autoclave and heated 72 h at 448 K. The resulting black solid was washed with distilled water and dried for 12 h at 353 K. It was first calcined in air at 553 K for 2 h and then under nitrogen flow at 873 K for 2 h. For *M1* (Sb), 2.12 g of ammonium heptamolybdate was dissolved in 30 mL of distilled water at 353 K. Then 0.53 g of antimony sulfate powder was slowly added and the solution was vigorously stirred for 15 min. Finally, an aqueous solution containing 5.26 g of hydrated vanadyl sulfate dissolved in 15 mL of distilled water was added. The slurry was introduced into the autoclave and heated at 448 K for 24 h. The formed solid was separated from the solution, washed with water, dried at 313 K overnight, calcined in air at 553 K for 2 h and under nitrogen flow at 873 K for 2 h.

Powder X-ray diffraction (XRD) patterns were obtained using a BRUKER D5005 diffractometer and Cu Kα radiation. They were recorded with 0.02° (2*θ*) steps over the 3–80° angular range with 1 s counting time per step. Metal contents of the solids were determined by atomic absorption (ICP).

The surface acidity of the catalysts was investigated by means of a Fourier transform infrared spectroscopic (FT-IR) study of pyridine adsorption. Pyridine FT-IR spectra were recorded in a IFS110 BRUKER spectrometer (DTGS detector). The samples were pressed into self-supporting discs (40–50 mg, 18 mm diameter), placed in an IR cell, and treated at 523 K under vacuum (10^{-5} Torr or 0.0013 Pa) for 2 h. After cooling to room temperature, the samples were exposed to pyridine vapor for 5 min (vapor pressure 3.3 kPa). Then, the spectra (200 scans, resolution: 1 cm^{-1}, range of acquisition: 1000–4000 cm^{-1}.) were recorded after evacuation (10^{-5} Torr or 0.0013 Pa) for 30 min at 298, 373, 423, 473, 523 and 573 K.

The oxidation of propane was performed in a fixed bed reactor operating at atmospheric pressure under conditions described elsewhere [7]. The catalytic properties were determined between 583 K in a conventional flow reactor with a catalyst mass varying from 0.5 to 1 g. The molar feedstock composition was $O_2/C_3H_8/H_2O/N_2/He$ = 10/5/45/35/5 with GHSV = 2500 h^{-1}. The reactants and gas products were analyzed with an on-line gas chromatograph using Porapak-Q and CP-Molsieve 5 Å columns. The organic substrates were condensed during the reaction and analyzed off line. Products formed under our reaction conditions were propene, CO, CO_2, acetone, acetic and acrylic acids. Traces of acrolein have been observed but not considered for calculations. The catalytic tests were conducted for at least 12 h and the catalysts were recovered after catalytic test by cooling them down rapidly in the flow of reactants from 653 K. Carbon balance based on the products listed above was satisfactory in all runs within 100 ± 2%.

3. Results and discussion

The results of the chemical analysis of the prepared *M1* phases are presented in Table 1. The cationic ratios obtained from chemical analysis were relatively close to each other. The phases that did not contain Nb were richer in vanadium as expected. The Te(Sb)/M ratio (with M = Mo + V + Nb) corresponded well to the theoretical one with however for the Nb containing phases a slight Te and Sb substoichiometry. The X-ray diffraction patterns of the prepared compounds are displayed in Fig. 1. All the solids were well crystallized and contained only one phase.

The nature of acid sites (Lewis and Brønsted) on the surface of the catalysts has been studied by FT-IR spectroscopy of pyridine adsorption. The spectra arising from pyridine adsorption at room temperature followed by evacuation at the same temperature are shown in Fig. 2. The bands at 1610, 1575, 1490, 1446 and 1596 cm^{-1} have been assigned to the vibrational modes of Lewis site coordinated pyridine [17]. Similarly, the bands at 1640, 1576, 1490 and 1538 cm^{-1} correspond to a pyridinium ion bonded to a Brønsted site. The bands around 1490 and 1576 cm^{-1} are associated at the same time to both Brønsted and Lewis acid sites. In addition to these peaks, FT-IR spectra showed also peak at 1437 and 1584 cm^{-1} corresponding to physisorbed pyridine. All the bands reported above were observed in the spectra recorded at room temperature. Fig. 3 shows the Brønsted and Lewis relative acidity of the *M1* phases, expressed as area under the peak at 1540 and 1450 cm^{-1}, normalized by surface unit in the spectra recorded after desorption at 373 K. Fig. 4 shows the evolution of the acidity as a function of temperature between 373 and 600 K. Upon out-gassing at increasing temperatures, the intensities of all the bands decreased.

No more Brønsted acid sites were detected at 373 K on the catalysts containing tellurium and no Lewis acid sites were neither detected on the *M1*(Te–Nb) sample.

Table 1
Results of the chemical analyses of the synthesized *M1* phases

Compound	Chemical analysis
M1(Te–Nb)	$MoV_{0.26}Te_{0.11}Nb_{0.12}$
M1(Sb–Nb)	$MoV_{0.28}Sb_{0.13}Nb_{0.15}$
M1(Te)	$MoV_{0.51}Te_{0.17}$
M1(Sb)	$MoV_{0.46}Sb_{0.17}$

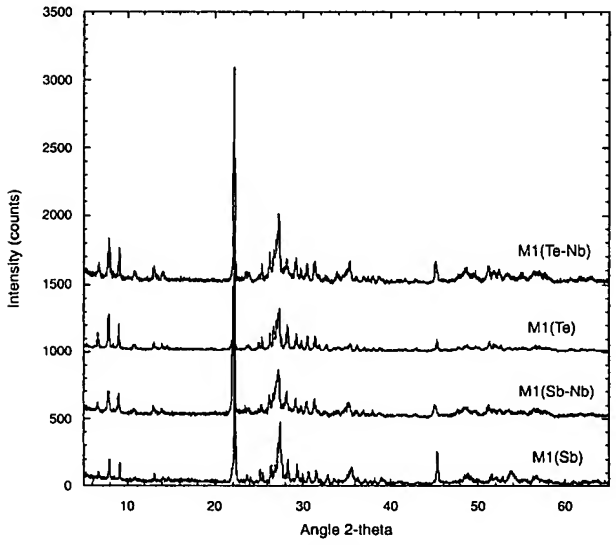

Fig. 1. X-ray diffraction patterns of the *M1* phases.

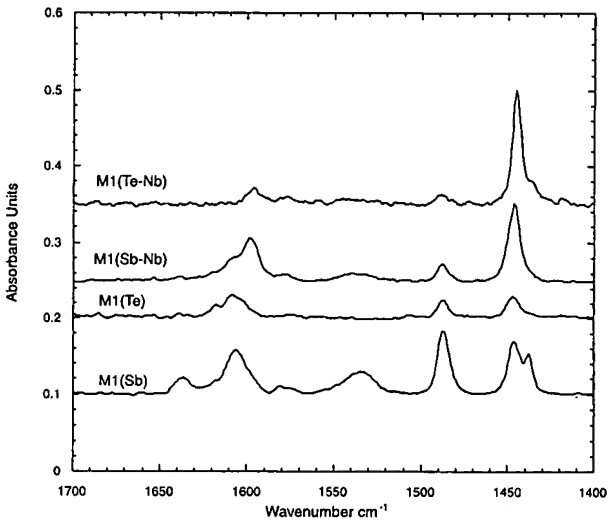

Fig. 2. FT-IR spectra of the surface species after pyridine adsorption and outgassing at 298 K on the *M1* phases.

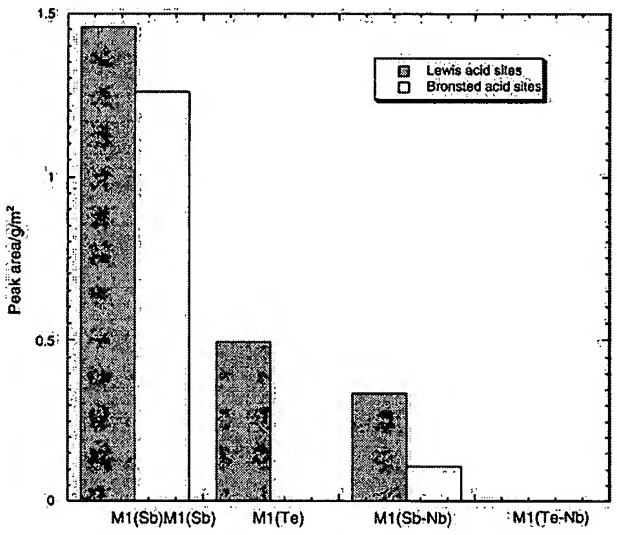

Fig. 3. Comparison of the Brønsted and Lewis relative acidity of the *M1* phases, expressed as area under the peak at 1540 and 1450 cm^{-1} normalized by surface unit in the spectra recorded after desorption at 373 K.

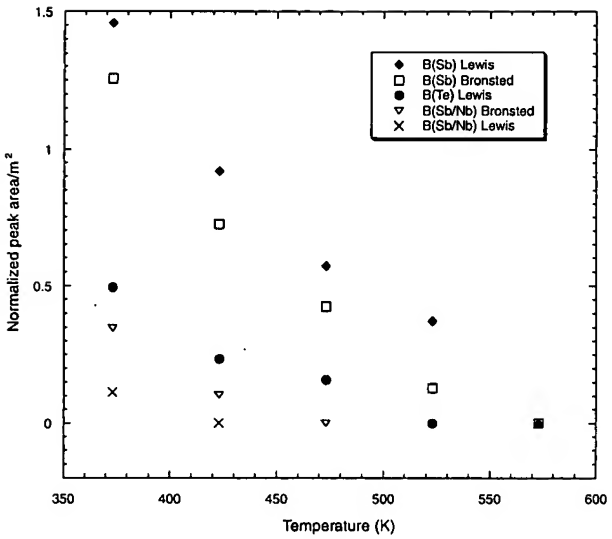

Fig. 4. Variation of the Brønsted and Lewis relative acidity of the *M1* phases, expressed as area under the peak at 1540 and 1450 cm^{-1} normalized by surface unit as a function of temperature.

The later phase appeared thus with both a very low Brønsted and Lewis acidity. By increasing further the desorption temperature above 373 K both Brønsted and Lewis acid sites remained in the *M1*(Sb) and *M1*(Sb–Nb) samples. Concerning the Brønsted sites, it is important to note that the protonation of a relatively weak base such as pyridine is an indication of their relevant strength. The stability of the pyridinium cations even after evacuation at 523 K is a further indication that the sites were rather strong on Sb containing catalysts. The number and strength of Lewis acid sites decreased in the order *M1*(Sb) > *M1*(Te) > *M1*(Sb–Nb) > *M1*(Te–Nb) whereas the number and strength of Brønsted acid sites followed the trend: *M1*(Sb) > *M1*(Sb–Nb) > *M1*(Te) > *M1*(Te–Nb). A slight variation in position of the band at 1540 cm^{-1} over a range of 5 cm^{-1} in the solids following the same order was observed. For the same type of phase, it is important to point out that the incorporation of niobium led to a decrease of the amount and the strength of both types of acid sites.

The catalytic performances of the phases in propane oxidation to acrylic acid have been determined at 653 K (Table 2). All catalysts showed almost the same activities in propane oxidation and gave acrylic acid, propene, acetic acid and CO_x. Formation of acetone in small amount was mainly observed on *M1*(Sb). Since conversions were almost the same, the selectivity sets obtained could be compared. The *M1*(Te–Nb) appeared to be the most selective catalyst to acrylic acid which was in agreement data reported previously [12,18]. For catalysts containing antimony we observed the same effect: the presence of niobium led to an increase of acrylic acid selectivity but in this case, *M1*(Sb) also presented high

Table 2
Catalytic properties of the *M1* phases at 653 K

Compound	Conversion (%)	Selectivities (%)				
		CO_x	C_3H_6	AA	Ace	AcA
M1(Sb)	29	37	15	26	2	20
M1(Te)	29	29	13	48	0	10
M1(Sb–Nb)	31	24	11	52	0	8
M1(Te–Nb)	31	22	11	58	0	9

Reaction conditions: feedstock composition $O_2/C_3H_8/Ne/N_2/H_2O$ = 3/1.5/1.5/10.5/13.5; total flow = 30 mL/min; catalyst mass = 0.50 g. AA, acrylic acid; Ace, acetone; AcA, acetic acid.

selectivity to acetic acid. The selectivity in acrylic acid decreased in the order *M1*(Te–Nb) > *M1*(Sb–Nb) > *M1*(Te) > *M1*(Sb).

Before discussing the results obtained and trying to find correlations between acidity and catalytic properties, it is interesting to recall the proposed reaction mechanism for the oxidation of propane on these catalysts [19]. The activation of propane by surface V=O· moeties has been proposed. Such H-atom abstraction from and alkane by a O-radical center has already been proposed in several cases [20,21]. The formed propyl radical would loose a second hydrogen presumably on a Te–O center to form a propene molecule. It has been shown that the oxygen atoms bound only to Te cations would also have a radical character facilitating this second abstraction [5]. Afterwards the reaction mechanism should follow thus already described for the transformation of propene into acrylic acid [22]. It is reasonable to think that the acidity of the surface will strongly affect the binding and reactivity of propene molecules which have a basic character.

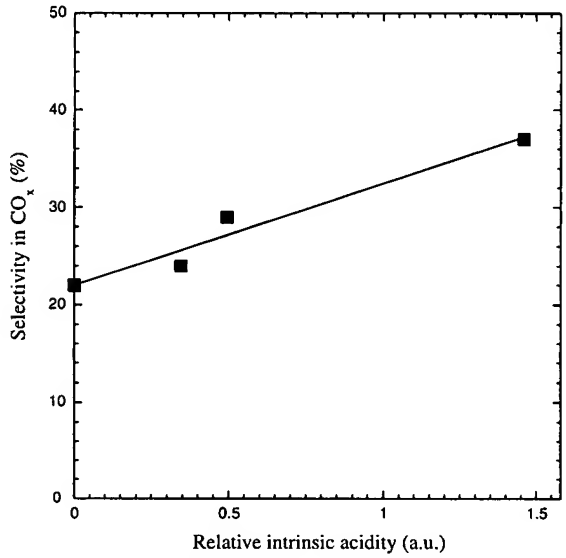

Fig. 5. Correlation between the selectivity in CO_x at 803 K and the number of Lewis acid sites identified by pyridine adsorption at 378 K on the different *M1* phases.

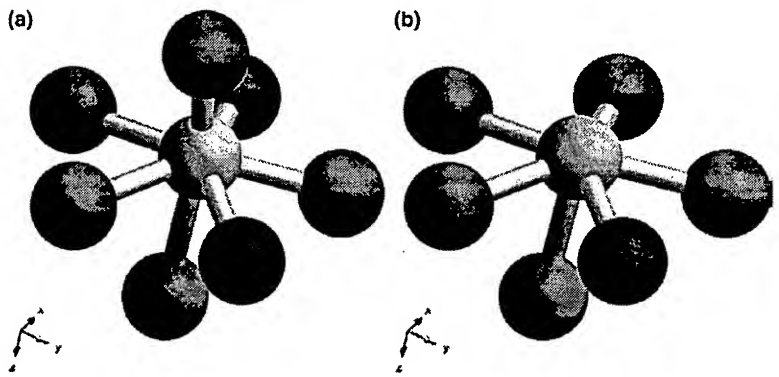

Fig. 6. Oxygen coordination of the Nb (a) and V or Mo (b) in the active plane (0 0 1) plane of the *M1* phase. The five oxygen surrounding the V or Mo cations are in the plane. The cations should be located below this plane closed to the sixth oxygen.

The two catalysts containing Te have few and very weak Brønsted acid sites (Figs. 3 and 4). The presence of niobium affected thus mainly the number and strength of Lewis sites that both decreased. In the same time an increase of selectivity in acrylic acid was observed (Table 2). The increase is mainly obtained to the depends of the selectivity in CO_x. On stronger Lewis acid centers, propene is more strongly adsorbed which results in prolongation of the residence time of propene molecules at the surface which increases the probability of an electrophylic attacks of adsorbed oxygen and combustion of the molecules. Fig. 5 shows a linear correlation between the selectivity in CO_x at 653 K and the number of Lewis acid sites identified by pyridine adsorption at 373 K on the different *M1* phases. It is interesting to note that the contribution to the formation of CO_x from propene represented a little less than the half. CO_x should also be formed by the oxidation of other adsorbed intermediates or products (acrolein, acetone, acetic and acrylic acids,...).

The presence of niobium in the antimony containing phase has an effect both the Lewis and Brønsted acidity that both decreased. Again an increase of acrylic acid selectivity was observed. But in this case this increase occurred not only to the depends of that in CO_x but also to that in acetic acid. This may be explained by the fact that on Brønsted acid center carbonium ion mechanism may operate in the transformation of propene [23]. This would result in the formation of propoxide type adsorption complexes. In the presence of water the complexes decompose to produce isopropyl alcohol and regenerate surface acid centers. At high temperature and in the presence of redox centers on the catalyst surface, dehydrogenation of isopropyl alcohol follows easily its formation resulting in the appearance of acetone and further oxidation to acetic acid.

When putting in relation the results of acidity characterization and of catalytic testing, a correlation between the selectivity of the catalysts and their acidity was observed. On the contrary, the activity of the catalysts remained almost the same, which indicated that the acidity does not affect the propane activation. Neither does the presence of niobium. This later conclusion had already been reached [24]. Niobium cations have been shown to occupy a specific site in the structure of the *M1* phase [9]. This site is mainly located in the pentagonal channels and it exhibits a rather unusual heptagonal coordination (bi-pyramid with pentagonal base) (Fig. 6). The d_0 cations, V^{5+} and Mo^{6+} cations that occupy this site should accommodate the coordination uncompletely leading to rather strong Lewis acid sites responsible for total oxidation in the (0 0 1) plane perpendicular to the channels shown to be the active plane. Calculations will be undertaken in order to ascertain this conclusion. The presence of niobium and the control of the preparation parameters allowing to avoid the occupation of the pentagonal channel of the *M1* phase structure by other cations than niobium are key parameters to high selective catalyst.

Acknowledgement

Dr. Ueda (Catalysis Research Center, Hokkaido, Japan) is gratefully thanked for providing hydrothermally synthesized catalysts.

References

[1] T. Ushikubo, K. Oshima, T. Ihara, H. Amatsu, US Patent 5,534,650, 1996, assigned to Mitsubishi Chemical Co.
[2] T. Ushikubo, K. Oshima, A. Kayou, M. Vaarkamp, M. Hatano, J. Catal. 169 (1997) 394.
[3] T. Ushikubo, K. Oshima, A. Kayou, M. Hatano, in: C. Li, Q. Xin (Eds.), Studies in Surface Science and Catalysis, vol. 112, Elsevier, 1997, p. 473.
[4] R.K. Grasselli, Top. Catal. 15 (2,4) (2001) 93.
[5] J.M.M. Millet, H. Roussel, A. Pigamo, J.L. Dubois, J.C. Jumas, Appl. Catal. A 232 (2002) 77.
[6] J.M.M. Millet, M. Baca, A. Pigamo, D. Vitry, W. Ueda, J.L. Dubois, Appl. Catal. A 244 (2) (2003) 359.
[7] M. Baca, A. Pigamo, J.L. Dubois, J.M.M. Millet, Top. Catal. 23 (1–4) (2003) 39.

[8] M. Baca, J.M.M. Millet, Appl. Catal. A, 2005, in press.
[9] P. DeSantro Jr., D.J. Buttrey, R.K. Grasselli, C.G. Lugmair, A.F. Volpe Jr., B.H. Toby, T. Weingand, T. Vogt, Top. Catal. 23 (1–4) (2003) 23.
[10] P. DeSanto Jr., D.J. Buttrey, R.K. Grasselli, C.G. Lugmair, A.F. Volpe Jr., B.H. Toby, T. Weingand, T. Vogt, Z. Kristallogr. 219 (2004) 152.
[11] W. Ueda, K. Oshihara, Appl. Catal. A 200 (2000) 135.
[12] P. Botella, B. Solsona, A. Martinez-Arias, J.M. Lopez-Nieto, Catal. Lett. 74 (2001) 149.
[13] M.M. Lin, Appl. Catal. A 207 (2001) 1.
[14] D. Vitry, Y. Morikawa, J.L. Dubois, W. Ueda, Appl. Catal. A 251 (1) (2003) 411.
[15] J.L. Dubois, S. Serreau, J. Jacquel, Patent 2 833 005 Fr, 2001, assigned to Atofina.
[16] J.L. Dubois, S. Serreau, French Patent FR2844263, 2002, assigned to Atofina.
[17] G. Busca, Phys. Chem. Chem. Phys. 1 (1999) 723.
[18] B. Solsona, J.M. Lopez-Nieto, J.M. Oliver, J. Gumbau, Catal. Tod. 91–92 (2004) 247.
[19] R.K. Grasselli, J.D. Burrington, D.J. Buttrey, P. DeSanto Jr., C.G. Lugmair, A.F. Volpe Jr., T. Weingand, Top. Catal. 23 (1–4) (2003) 5.
[20] A. Andersson, S.L.T. Andersson, G. Centi, R.K. Grasselli, M. Sanati, F. Trifiro, in: L. Guczi, F. Solymosi, P. Tetenyi (Eds.), Proceedings 10th Int. Cong. Catal., Akademiai Kiado, Budapest, 1992, p. 691.
[21] H. Bluhm, M. Haevecker, E. kleimenov, A. Knope-Gericke, A. Liskowski, R. Sloegel, D. Su, Top. Catal. 23 (1–4) (2003) 109.
[22] R.K. Grasselli, in: G. Ertl, H. Knözinger, J. Weitkamp (Eds.), Handbook of Heterogeneous Catalysis, vol. 5, Wiley-VCH, New York, 1997, p. 2307.
[23] Y. Moro-oka, Y. Takita, A. Ozaki, J. Catal. 12 (1968) 241.
[24] T. Katou, D. Vitry, W. Ueda, Catal. Tod. 91–92 (2004) 241.

Available online at www.sciencedirect.com
SCIENCE DIRECT
ELSEVIER
Applied Catalysis A: General 278 (2004) 45–56
APPLIED CATALYSIS A: GENERAL
www.elsevier.com/locate/apcata

Catalytic and FT-IR study on the reaction pathway for oxidation of propane and propylene on V- or Mo–V-based catalysts

P. Concepción, P. Botella, J.M. López Nieto*

Instituto de Tecnología Química, UPV-CSIC, Avenida de los Naranjos s/n, 46022-Valencia, Spain

Received 30 June 2004; received in revised form 6 September 2004; accepted 16 September 2004

Abstract

A series of V- and Mo–V-based catalysts, i.e. undoped and K-doped VO_x/Al_2O_3, MoVNbO, MoVSbO and MoVTeNbO mixed metal oxides, have been tested in the oxidation of propane and propylene. All the catalysts are active and relatively selective in the partial oxidation of propane and propylene, although the nature of reaction products changes depending on the characteristics of the catalysts. Thus, acrylic acid (MoVTeNbO), acetic and acrylic acid (MoVSbO), acetic acid (MoVNbO) and propylene and CO_x (supported catalysts) were the most important products obtained from both propane and propylene. FT-IR spectroscopy of NH_3 indicates the presence of Brønsted and Lewis acid sites, although the acidity decreases in the order: MoVNbO > VO_x/Al_2O_3 > MoVSbO > MoVTeNbO > K-doped VO_x/Al_2O_3. FT-IR studies of propylene adsorbed and desorbed at different temperatures allowed us to propose three different intermediates: (i) a π-allylic compound, intermediate in the selective oxidation of propylene to acrylic acid; (ii) an enolic-type compound, intermediate in the hydration/oxidation of the olefin to form acetone and acetic acid; (iii) a π-bonded propylene species interacting with Lewis acid sites, precursor in the deep oxidation of propylene. Accordingly, the key factors in the achievement of an active and selective catalyst for the oxidation of propane to acrylic acid as MoVTeNbO mixed oxides is tentatively proposed. The role of acid sites in selective and non-selective pathways are also discussed.

Keywords: Mo–V–Te–Sb–Nb mixed oxide catalysts; Alumina-supported vanadia; Selective oxidation of propane and propylene to acrylic acid, acetic acid; Catalyst characterization (XRD, XPS, FT-IR of ammonia or propylene adsorbed)

1. Introduction

In the past decade there has been a great interest in the development of highly active and selective catalysts for partial oxidation of light alkanes due to their potential application as a source of cheap raw materials. In fact, the direct conversion of light alkanes into various products, i.e. olefins, or aldehydes, acids and nitriles α,β-unsaturated, is one of the most challenging problems in petrochemistry since it can enable natural gas to be used as the feedstock for producing, in large scale, chemicals currently obtained from oil [1–9].

Mixed metal oxides catalysts, i.e. bulk or supported metal oxides, are an important class of catalytic materials in the selective oxidation of alkanes. Supported vanadia catalysts have been proposed as one of the most interesting catalytic systems in the oxidative dehydrogenation (ODH) of short chain alkanes [1,6–9], although their catalytic performance depends strongly on the acid character of both support and catalysts and the alkane feed [6]. Thus, it has been observed that the ODH of ethane on V-containing catalysts is selectively carried out on catalysts with acid character [6,7], while the ODH of butane on V-containing catalysts is more effective on basic catalysts [7]. A clear example is the incorporation of potassium on the surface of VO_x/Al_2O_3 catalysts, which has a promoter effect during the ODH of propane [10] or

* Corresponding author. Tel.: +34 963877808; fax: +34 63877809.
E-mail address: jmlopez@itq.upv.es (J.M. López Nieto).

0926-860X/$ – see front matter © 2004 Elsevier B.V. All rights reserved.
doi:10.1016/j.apcata.2004.09.024

n-butane [11,12] but a negative effect during the ODH of ethane [11].

Bulk mixed metal oxides have been proposed as selective in the O- and N-insertion reactions [1–5]. In this way, bulk V–Mo-containing mixed metal oxide catalysts have been proposed during the last decade as one of the most selective catalysts in the selective oxidation of light alkanes [1–5,13–33].

Mo–V–Nb–O mixed metal oxides were proposed as active and selective catalysts in the ODH of ethane [13–16] although they present a relatively low selectivity from propane [17,18]. The appearance of several reaction products by consecutive reactions from propane [17] which are not observed from ethane, could partially explain the catalytic performance of this catalytic system from both alkanes.

Mo–V–Nb–Te–O mixed metal oxide catalysts have been proposed in the last years as the most active and selective in the ammoxidation of propane to acrylonitrile [2–5,19–24], the selective oxidation of propane to acrylic acid [2–5,25–27], and in the oxidative dehydrogenation of ethane to ethylene [28,29]. The presence of Te-containing crystalline phases facilitates the selective consecutive reactions from propylene (favouring the formation of acrylic acid or acrylonitrile) during the oxidation of propane [19–27].

Mo–V–Nb–Sb–O mixed metal oxide catalysts have recently been proposed as active and selective catalysts in the oxidation of propane to acrylic acid [30–33], although the main of the scientific papers report a relatively low selectivity to acrylic acid [31–33]. Recently, it has been proposed that the incorporation of potassium ions on the surface of MoVSbO catalysts could enhance the selectivity to acrylic acid [33] by the elimination of the Brønsted acid sites on the catalyst surface. So, the nature and strength of acid sites, in addition to the chemical composition of the catalyst, could have a strong influence on the nature of reaction products during the selective oxidation of propane.

In the present study, we investigated five different V-containing catalysts, active and selective in the propane activation, in which different reaction products can be achieved: (i) VO_x/Al_2O_3 catalyst active but poorly selective in the ODH of propane; (ii) K-doped VO_x/Al_2O_3 catalyst active and relatively selective in the ODH of propane; (iii) Mo–V–Nb–O mixed metal oxides catalyst active and relatively selective in the ODH of propane; (iv) Mo–V–Sb–O mixed metal oxide catalyst active and relatively selective in the oxidation of propane to acetic and acrylic acids; and (v) Mo–V–Te–Nb–O mixed metal oxides catalysts active and very selective in the oxidation of propane to acrylic acid. A correlation between the characteristics of acid sites in each catalyst (determined from the FT-IR spectra of ammonia adsorbed and desorbed at different temperatures) and the nature of reaction intermediates (determined from the FT-IR spectra of propylene adsorbed and desorbed at different temperatures) can be proposed.

2. Experimental

2.1. Catalyst preparation

Supported vanadia catalysts have been prepared by "wet" impregnation of alumina (Gidler T126 γ-Al_2O_3 support; $S_{BET} = 188\ m^2\ g^{-1}$) with an aqueous solution of ammonium metavanadate (undoped VO_x/γ-Al_2O_3 sample) or ammonium metavanadate/potassium carbonate in order to achieve a K/V atomic ratio of 0.7 (K-doped VO_x/γ-Al_2O_3 sample) [10]. The solids were dried at 80 °C for 4 h and 27 kPa and then kept at 110 °C for 16 h. Finally, they were calcined in air at 600 °C for 4 h. The samples will be named as VAl-1 and KVAl-2.

Bulk Mo–V–Nb–O mixed metal oxide catalyst has been prepared from an aqueous solution of ammonium heptamolybdate, vanadyl sulphate and niobium oxalate [16]. The aqueous solution is evaporated in a rotavapor. The solid was dried at 100 °C overnight and finally heat-treated at 450 °C in N_2 during 4 h. The catalysts will be named as MoVNb-3.

Bulk Mo–V–Sb–O and Mo–V–Te–Nb–O mixed metal oxides catalyst has been prepared hydrothermally. Ammonium heptamolybdate, vanadyl sulfate, antimony sulphate, niobium oxalate, and telluric acid, have been used as reagents. Mo/V/Sb atomic ratio of 0.75–0.14–0.11 was used in the preparation of a Mo–V–Sb mixed metal oxide catalyst [33], while Mo/V/Te/Nb atomic ratio of 0.65–0.13–0.11–0.11 was used in the preparation of a Mo–V–Te–Nb mixed metal oxide catalyst [26]. The gels were autoclaved in Teflon-lined stainless-steel autoclaves at 175 °C for 96 h (MoVSb) or 48 h (MoVTeNb). The resulting precursors were filtered, washed, dried at 80 °C for 16 h and calcined at 600 °C during 2 h in N_2-stream. These samples will be named as MoVSb-4 and MoVTeNb-5, respectively. The characteristics of catalysts are presented in Table 1.

2.2. Catalytic tests

The catalytic experiments were carried out in an isothermal fixed-bed tubular reactor, working at atmospheric pressure, and equipped with a coaxial thermocouple for catalytic bed temperature profiling. Catalyst samples (0.3–0.5 mm particle size) were introduced in the reactor. The flow rate and the amount of catalyst were varied in order to obtain different hydrocarbon conversion levels. The feed consisted of a mixture of propane (or propylene)/oxygen/water/helium with a molar ratio 4/8/30/58. Experiments were carried out in the 320–400 °C temperature interval. Reactants and reaction products were analysed by on-line gas chromatography [26].

2.3. Catalyst characterization

BET specific surface areas were measured on a Micromeritics ASAP 2000 instrument (adsorption of

Table 1
Characteristics of V-containing catalysts

Sample	Chemical composition[a]	V-content (wt.% V-atoms)	S_{BET} ($m^2\ g^{-1}$)	XRD phases	XPS results[b]		
					V^{5+}/V^{4+}	Mo^{6+}/Mo^{5+}	Surface atomic ratio
VAl-1	$Al_1V_{0.08}O_x$	3.5	137	γ-Al_2O_3	10.20	–	$Al_1V_{0.14}$
KVAl-2	$Al_1V_{0.08}K_{0.06}O_x$	3.5	138	γ-Al_2O_3	6.00	–	nd
MoVNb-3	$Mo_1V_{0.41}Nb_{0.14}O_x$	11.4	24	$Mo_6V_9O_{40}$, $Mo_4V_6O_{25}$	0.26	0[c]	$Mo_1V_{0.30}Nb_{0.14}$
MoVSb-4	$Mo_1V_{0.19}Sb_{0.17}O_x$	4.8	9	$Sb_4M_{10}O_{30}$[d], $Sb_2M_{10}O_{31}$[d]	0.15	2.29	$Mo_1V_{0.19}Sb_{0.08}$
MoVTeNb-5	$Mo_1V_{0.21}Te_{0.17}Nb_{0.17}O_x$	4.2	15	$Te_2M_{20}O_{57}$[e], $Mo_{5-x}(V/Nb)_xO_{14}$, $Te_{0.33}MO_{3.33}$[e]	0.18	1.35	$Mo_1V_{0.18}Te_{0.19}Nb_{0.19}$

[a] The atomic ratios of calcined samples were determined by atomic absorption spectroscopy.
[b] Binding energies (and FWHM) determined by XPS: V^{5+}, 517.5 eV (1.25 eV); V^{4+}, 516.4 eV (1.75 eV); Mo^{6+}, 232.8 eV (1.75 eV); Mo^{5+}, 231.8 eV (1.75 eV); Sb^{3+}, 539.5 eV (1.37 eV); Nb^{5+}, 206.5 eV (1.76 eV); Te^{4+}, 576.3 eV (1.78 eV); Al^{3+}, 73.98 eV (2.39 eV).
[c] A peak at 232.1 eV (1.78 eV) related to Mo^{5+} is only observed.
[d] $Sb_4M_{10}O_{30}$ and $Sb_2M_{10}O_{31}$ (with M = Mo and V).
[e] $Te_2M_{20}O_{57}$ and $Te_{0.33}MO_{3.33}$ (with M = Mo, V and Nb).

krypton) and on a Micromeritics Flowsorb apparatus (adsorption of N_2).

X-ray diffraction patterns (XRD) were collected using a Philips X'Pert diffractometer equipped with a graphite monochromator, operating at 40 kV and 45 mA and employing nickel-filtered Cu Kα radiation (λ = 0.1542 nm).

X-ray photoelectron spectra (XPS) were recorded on a VG-Escalab-210 electron spectrometer using Al Kα radiation (Al Kα = 1486.6 eV) of a twin anode in the constant analyser energy mode, with a pass energy of 50 eV. The samples in the form of self-supporting wafers of 13 mm diameter were outgassed overnight in the preparation chamber of the spectrometer and subsequently transferred to the analysis chamber. The pressure of the main chamber during spectra acquisition was maintained at ca. 1.0×10^{-9} mbar. The binding energy (BE) scale was regulated by setting the C 1s transition at 284.6 eV. The accuracy of the BE was ±0.1 eV. Data analysis procedure involve smoothing, a Shirley background subtraction and curve fitting using mixed Gaussian–Lorentzian functions by a least-squares method. Atomic ratios of elements were calculated from the relative peak areas of the respective core level lines using Wagner sensitivity factors [34]. The integration of the V $2p_{3/2}$ core level line is influenced by the Kα3,4 satellite subtraction of the O 1s line. Therefore, the satellite subtraction (intensity ratios I/I_0 and energies distances ΔE between main line and satellite) have been adjusted by using a reference material without vanadium in order to obtain a smooth background baseline. The Sb $3d_{5/2}$ peak almost overlaps with that of O 1s, thus the Sb $3d_{3/2}$ transition has been used for both quantitative analysis of the Sb composition and for the identification of the chemical state of the Sb.

IR spectra have been recorded with a BioRad, FTS-40A FT-IR spectrophotometer, by using a conventional quartz infrared cell connected to a vacuum dosing system. The catalyst powder was pressed into self-supporting disc and activated at 200 °C in vacuum for 1 h, before adsorption experiments. Adsorption of NH_3 (32 mmol g^{-1}) was performed at room temperature (rt), followed by evacuation

Table 2
Propane oxidation on V-based catalysts

Sample	Temperature (°C)	W/F[a]	Conversion (%)[b]	Selectivity (%)					
				C_3H_6	Acrylic acid	Acetic acid	Acetone	CO	CO_2
VAL-1	340	500	7.8	41.1	–	–	0.1	15.7	43.0
	380	500	26.1	23.0		–	0.1	26.7	50.2
KVAl-2	380	500	4.1	49.2	–	–	0.7	9.6	40.5
	420	1000	26.8	28.9	–	–	0.1	16.7	54.2
MoVNb-3	300	150	6.5	28.9	–	10.9	0.7	23.1	36.4
	300	500	20.4	4.3	–	19.8	0.3	35.7	39.9
	340	500	50.6	1.9	–	2.8	1.1	41.6	52.6
MoVSb-4	360	200	11.8	16.0	6.2	18.4	3.1	20.5	36.0
	360	500	29.5	9.2	8.4	12.7	0.7	25.9	43.1
MoVTeNb-5	360	200	7.9	26.6	49.6	5.8	3.7	6.3	8.0
	360	500	19.4	8.8	60.0	9.9	2.2	7.8	11.1
	380	500	48.3	3.0	58.0	5.3	0.2	11.3	22.2

[a] Contact time, W/F, in g_{cat} h $mol^{-1}_{C_3H_8}$.
[b] $C_3H_8/O_2/He/H_2O$ molar ratio of 4/8/58/30.

at the same temperature in order to remove physisorbed NH_3. Under these conditions, spectra at 25 °C and after increasing the temperature to 100 °C have been collected. In all cases FT-IR spectra of the unloaded catalyst sample were recorded as reference spectrum, which was subtracted from the obtained spectrum after adsorption of the gases. NH_3 adsorption spectra has been normalized according to both the sample weight and the sample surface area. Adsorption of propylene (17 mmol g^{-1}) was carried out at room temperature for 1 h, followed by increasing the temperature to 100, 150, 200 and 250 °C, with stabilization times of 1 h at each temperature.

3. Results

3.1. Propane and propylene selective oxidation

Table 2 presents the catalytic results obtained during the oxidation of propane on V-containing catalysts. Bulk mixed metal oxide catalysts present higher catalytic activity than supported vanadium oxide catalysts. Although one could concluded that V species in bulk catalysts are more active in propane activation than those present in supported vanadia catalysts, it must be taken into account that the presence of other elements (especially Mo) could enhance the catalytic activity of V atoms in mixed metal oxides.

Propylene is the main partial oxidation product at very low propane conversions (Fig. 1), suggesting that this is initially formed from propane over our catalysts. In addition, it can also be seen that the best selectivity to partial oxidation products is obtained on the MoVTeNbO catalysts, with an initial selectivity to propene higher than 90%. However, carbon oxides are also observed at low propane conversion, suggesting that they are also partially formed from propane (see Scheme 1).

In the case of supported catalysts, the selectivity to propylene decreases at high propane conversion with the formation of carbon oxides. So, the deep oxidation of propylene can be proposed, as the consecutive reaction, on Al_2O_3-supported vanadia catalysts.

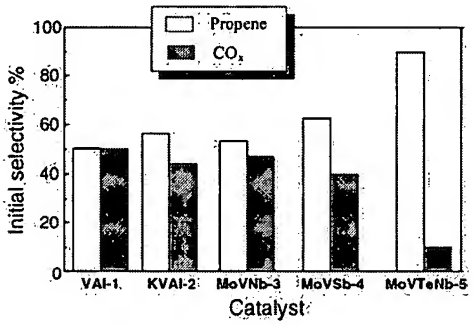

Fig. 1. Initial selectivities (at propane conversion near to 0) to the main reaction products, i.e. propylene and CO_x, obtained during the propane oxidation at 380 °C over: VAl-1, KVAl-2, MoVNb-3, MoVSb-4, MoVTeNb-5.

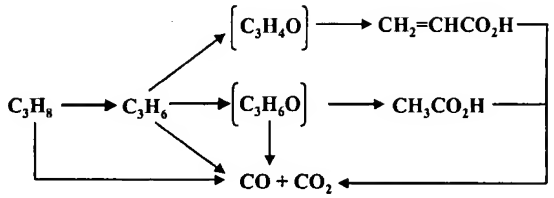

Scheme 1. Reaction network for the selective oxidation of propane on mixed metal oxides.

Over bulk catalysts, the selectivity to propylene decreases and the formation of carboxylic acids (acetic and/or acrylic acid) increases when increasing the propane conversion (Table 2). We must notice that the maximum of the selectivity to carboxylic acid is obtained for propane conversions of 30–40% [26,33]. In addition, the acrylic acid/acetic acid ratio changes in these catalysts suggesting different mechanisms in their formation. Moreover, we must inform that a yield of acrylic acid of about 35% has been obtained on MoVTeNb-5 sample working at 380 °C and a contact time, W/F, of 1000 g_{cat} h $mol_{C_3}^{-1}$.

In order to get a better understanding of the different pathways in the mechanism for propane oxidation, we have carried out some experiments of propylene oxidation, since propylene can be considered as intermediate in propane oxidation. Table 3 presents the catalytic results obtained in the oxidation of propylene on these catalysts. According to these results, it can be concluded that the catalysts studied here are also active in the oxidative activation of propylene, but differences in the nature of reaction products are observed too. Relatively high selectivity to acetone and/or acetic acid is observed at low reaction temperature over bulk MoVNb-3 and MoVSb-4 mixed metal oxides. Moreover, the highest selectivity to acrylic acid was observed on MoVTeNb-5 catalyst when working at 360–400 °C. In fact, a yield of acrylic acid about 50% can be obtained during propylene oxidation at 380 °C on MoVTeNb-5 catalyst, while the yield of carboxylic acids, mostly acetic acid, on MoVSb-4 and MoVNb-3 at the same reaction conditions was of 27.5 and 17.1%, respectively.

On the other hand, acrolein was observed, with low selectivity, during the oxidation of propane on both undoped and K-doped VO_x/Al_2O_3. However, no carboxylic acids were observed on these catalysts. We must indicate that a lower catalytic activity in propylene oxidation and a higher selectivity to acrolein is observed in the K-doped sample. This can be explained by a partial elimination of combustion sites after the incorporation of K ions [11,12], in good agreement with the results obtained during the oxidation of propylene on Na-free and Na-doped VO_x/TiO_2 catalysts [35].

3.2. Catalyst characterization

Table 1 summarizes the characteristics of catalysts. Low surface areas have been achieved for bulk mixed metal oxide

Table 3
Propylene oxidation on V-based catalysts

Sample	Temperature (°C)	Conversion (%)[a]	Selectivity (%)					
			Acrylic acid	Acrolein	Acetic acid	Acetone	CO	CO_2
VAl-1	340	7.7	–	4.6	–	6.0	23.5	65.9
	380	13.4	–	3.3	–	1.4	32.2	63.1
KVAl-2	380	1.0	–	14.7	–	2.8	6.5	76.0
MoVNb-3	320	35.9	–	0.2	38.9	14.0	15.4	31.5
	380	70.7	–	0.2	24.2	1.2	34.3	40.1
MoVSb-4	320	30.0	14.2	–	11.0	45.1	9.2	21.3
	380	63.3	26.0	–	17.5	11.7	15.5	29.3
MoVTeNb-5	320	30.3	42.7	–	1.9	48.0	3.4	3.6
	380	63.6	77.5	–	5.2	4.7	5.3	7.0

[a] $C_3H_6/O_2/He/H_2O$ molar ratio of 4/8/58/30.

catalysts, i.e. MoVNb-3, MoVSb-4 and MoVTeNb-5. However, relatively high surface areas were obtained for undoped and K-doped VO_x/Al_2O_3 catalysts (VAl-1 and KVAl-2, respectively).

No vanadium containing crystalline phases have been observed on the undoped and K-doped VO_x/Al_2O_3 catalysts, but previous characterization results suggest that tetrahedral V^{5+} species are mainly present on both undoped and K-doped catalysts [10–12].

XRD analyses of bulk catalysts suggest the formation of several crystalline phases (Fig. 2). The XRD pattern of MoVNb-3 sample suggests the presence of an amorphous material as well as less well-crystallized $Mo_6V_9O_{40}$ and $Mo_4V_6O_{25}$ phases [16], although the presence of MoO_2 can also be proposed (Fig. 2a) [14]. Sb-containing and Te-containing phases can be proposed in samples MoVSb-4 and MoVTeNb-5, respectively (Fig. 2, patterns b and c, respectively). $Sb_4M_{10}O_{31}$ and $Sb_2M_{10}O_{31}$ (M = Mo and V) phases, with crystal structures similar to those proposed for $Sb_4Mo_{10}O_{31}$ and $Sb_2Mo_{10}O_{31}$ [36] can be proposed in sample MoVSb-4 (Fig. 2b) in agreement to previous results [31,33]. Moreover, $Te_2M_{20}O_{57}$ (M = Mo, V, Nb), with orthorhombic symmetry [5,22,24,28], and isostructural with $Cs_x(Nb,W)_5O_{14}$ [37], has mainly been observed in MoVTeNb-5 sample, although the presence of small amounts of $Mo_{5-x}(V/Nb)_xO_{14}$ and $Te_{0.33}MO_{3.33}$ (M = Mo, V, Nb) can also been proposed (Fig. 2c) [26,28].

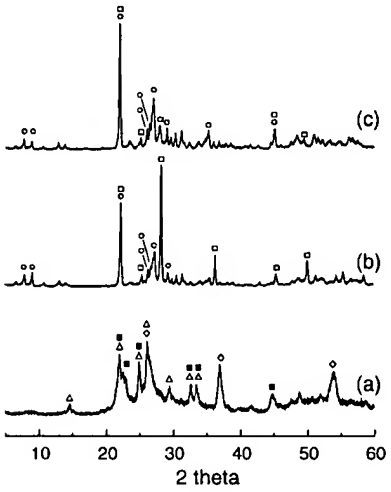

Fig. 2. XRD patterns of heat-treated samples: MoVNb-3 (a), MoVSb-4 (b), MoVTeNb-5 (c): (○) $Te_2M_{20}O_{57}$ or $Sb_2M_{10}O_{31}$; (□) $Te_{0.33}MO_{3.33}$ or $Sb_4Mo_{10}O_{31}$; (■) $Mo_6V_9O_{40}$; (△) $Mo_4V_6O_{25}$; (◇) MoO_2.

XPS has been used to provide information about the oxidation state and the chemical environment of the elements present on the surface of the catalysts (Table 1). Fig. 3A shows V $2p_{3/2}$ XP spectra of catalysts. Spectral deconvolution reveals the presence of two distinct V-environments, with the presence of two components at 516.4 and 517.5 eV and with full width at half maximum (FWHM) values of 1.75 and 1.25 eV, respectively. The component at lower BE corresponds to V^{4+}, while the higher BE component is related to V^{5+} sites [38,39]. On the other hand, the surface V^{5+}/V^{4+} atomic ratio of bulk catalysts was lower than those observed in supported catalysts (Table 1). In this way, the amount of V^{4+} species on the catalyst surface decreases in the following trend: MVSb-4 = MoVTeNb-5 > MoVNb-3 > KVAl-2 > VAl-1.

The Mo 3d core line spectra of Mo-containing catalysts are presented in Fig. 3B, where a broadening (FWHM = 2.05 eV) and a shift to higher BE (peak maxima at 232.5 eV) are observed in the Mo 3d lines of MoVSb-4

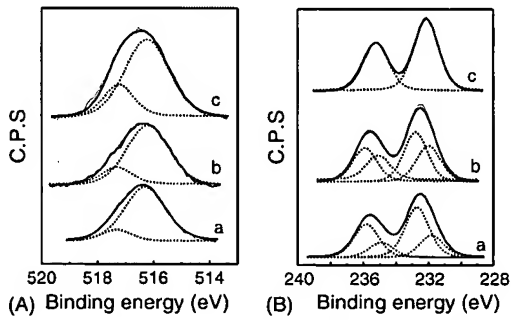

Fig. 3. V2p3/2 (A) and Mo3d (B) X-ray photoelectron spectra for, MoVNb-3 (a) MoVSb-4 (b), and MoVTeNb-5 (c) catalysts.

and MoVTeNb-5 samples. The FWHM of the Mo 3d line of the MoVNb-3 sample is 1.78 eV, and is shifted to lower BE 232.1 eV. Lower BE can be taken as indicative of species with lower oxidation states, independent of crystal size effects, i.e. relaxation effects and Madelung potential, while a higher FWHM is generally related to the presence of more than one component, taken into account the absence of charging effect in the sample. Curve fitting have been done in order to determine the presence of different Mo species and their relative amount. In this way, both Mo^{6+} (232.8 eV) and Mo^{5+} (231.8 eV) species are present in MoVSb-4 and MoVTeNb-5 samples, with Mo^{6+}/Mo^{5+} atomic ratios of c.a. 2.3 and 1.4, respectively (Table 1). The presence of niobium oxalate in the synthesis gel for the preparation of MoVTeNb-5 samples could favour an increase in the number of reduced Mo species [26].

In the case of the MoVNb-3 sample one component at 232.1 eV can only be inferred. This BE is 0.3 eV higher than the values attributed to Mo^{5+} sites in the other Mo-containing samples or those proposed by several authors [33,40], but similar to those reported by other authors for Mo^{5+} sites [41]. Independently of the controversy in the literature, the presence of reduced Mo species can be proposed in the MoVNb-3 sample, although the slightly higher BE (232.1 eV) observed in this case could be related to some variation of relaxation and/or Madelung potential of the sample.

According to these results, similar Mo^{6+}/Mo^{5+} and V^{5+}/V^{4+} atomic ratios are observed in both MoVSb-4 and MoVTeNb-5 samples, while V^{5+} sites and Mo sites with an oxidation state lower than 6 are mainly observed in the MoVNb-3 sample. Moreover, the Sb $3d_{3/2}$, Nb $3d_{5/2}$ and Te $3d_{5/2}$ core level lines are rather symmetric appearing at 539.5 eV (FWHM = 1.77), 206.5 eV (FWHM = 1.76) and 576.3 eV (FWHM = 1.78) binding energies, respectively. This suggests the presence of Sb^{3+} [31,32], Nb^{5+} [22], or Te^{4+} sites [22] on the surface of these catalysts.

3.3. FT-IR results on adsorption/desorption of NH_3

The nature of acid sites (Lewis and Brönsted) on the surface of the catalysts has been studied by IR spectroscopy of NH_3 as probe molecule. The spectra arising from NH_3 adsorption at room temperature followed by evacuation at the same temperature are shown in Fig. 4. Adsorption bands at 1618 and 1458 cm^{-1} corresponding to Lewis and Brønsted acid sites, respectively, can be observed in the undoped VAl-1 sample (Fig. 4, spectrum a) [10–12]. It has previously been shown by using CO [12] or pyridine [11] as probe molecules for acidity measurements that the incorporation of K in the KVAl-2 sample leads to a partial disappearance of both Lewis and Brønsted acid sites.

The IR spectra recorded after NH_3 adsorption at 25 °C and subsequent evacuation at the same temperature on MoVNb-3, MoVSb-4 and MoVTeNb-5 catalysts are also shown in Fig. 4 (spectra b–d). Adsorption of NH_3 on the

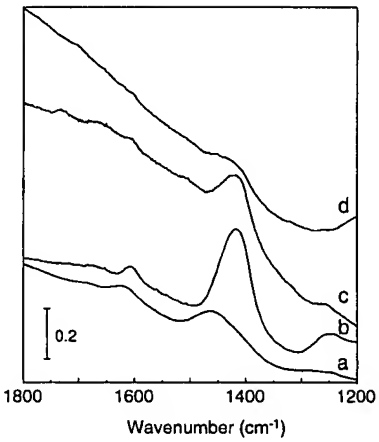

Fig. 4. FT-IR spectra of NH_3 adsorbed and desorbed at 25 °C on: VAl-1 (a), MoVNb-3 (b), MoVSb-4 (c), and MoVTeNb-5 (d).

MoVNb-3 and MoVSb-4 sample (Fig. 4, spectra b and c, respectively) leads to the appearance of a band at 1418 cm^{-1}, assigned to an asymmetric deformation vibration (δ_{as}) of the ammonium ions (NH_4^+) [42,43]. Conversely, the band at 1608 cm^{-1} is due to the asymmetric bending vibration for ammonia adsorbed on Lewis acid sites [43].

Adsorption and further desorption of NH_3 at 25 °C on MoVTeNb-5 sample (Fig. 4, spectrum d) shows a broad band centred at 1429 cm^{-1}, due to ammonium ions, and a weak band centred at 1608 cm^{-1}, due to ammonia coordinated to Lewis acid sites. The broadening of the IR band at 1429 cm^{-1} could be related to a non-homogeneity of Brønsted acid sites, or due to a splitting of the δ_{as} vibration due to the adsorption symmetry of the NH_4^+ molecule with the catalyst surface. Accordingly, the amount of acid sites decreases in the order MoVNb-3 > MoVSb-4 > MoVTeNb-5.

By increasing the temperature to 100 °C, the amount of both Brønsted and Lewis acid sites remain in the MoVNb-3 and MoVSb-4 samples, while only a low amount of Brønsted acid sites can be observed on the MoVTeNb-5 sample.

Thus, it can be concluded that both the amount and the strength of Lewis and Brønsted acid sites present in the MoVTeNb-5 sample are lower than those observed on the other samples. At this point, it must be taken into account that the presence of Te^{4+} could decrease the acid character of this catalyst in the same way than happens in Te-doped VPO catalysts [44]. Conversely, the higher presence of Brønsted acid sites observed in the MoVNb-3 sample could be related to the higher amount of Mo^{5+} species as determined from the XPS spectra.

3.4. FT-IR results on adsorption/desorption of propylene

The interaction of propylene with the surface of the catalysts have been studied by FT-IR spectroscopy at room temperature and at increasing temperatures in order to reveal

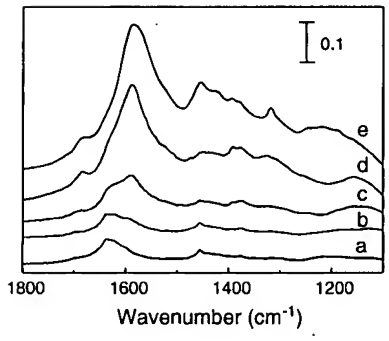

Fig. 5. FT-IR spectra of propylene adsorbed on VAl-1 sample at 25 °C (a); 100 °C (b); 150 °C (c); 200 °C (d); and 250 °C (e).

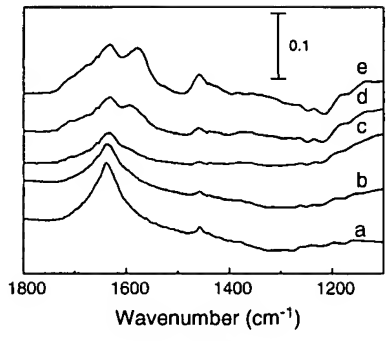

Fig. 6. FT-IR spectra of propylene adsorbed on KVAl-2 sample at 25 °C (a); 100 °C (b); 150 °C (c); 200 °C (d); and 250 °C (e).

surface intermediate species which allow a better understanding of the reaction mechanism pathway.

3.4.1. Adsorption of propylene on VO_x/Al_2O_3 catalyst

Fig. 5 shows the IR spectra of the VAl-1 catalyst after adsorption of propylene at room temperature and their evolution with the temperature. A band at 1636 with a broad shoulder around 1616 cm^{-1}, due to C=C stretching, together with other less intense bands at 1456 and 1374 cm^{-1}, associated to the asymmetric and symmetric – CH_3 deformation, are observed after propylene adsorption at room temperature [45]. These bands can be assigned to physisorbed propylene (νC=C, 1636 cm^{-1}) and propylene π-bonded to surface Lewis acid sites (νC=C, 1616 cm^{-1}) [45]. Increasing the temperature to 100 °C, a shoulder at 1584 cm^{-1} can be observed. The intensity of this band increases by increasing the temperature to 150–250 °C, together with an increase of intensity of the bands at 1456, 1374 cm^{-1} and the appearance of a new band at 1391 cm^{-1}. These bands can be assigned to a mixture of acetate ions (1580 and 1462 cm^{-1}) and formate ions (1395 and 1377 cm^{-1}) [45,46]. On the other hand, a band at 1680 cm^{-1} due to acetone species appeared at 200 °C.

3.4.2. Adsorption of propylene on K-doped VO_x/Al_2O_3 catalyst

The IR spectra of the KVAl-2 sample after propylene adsorption at room temperature and their evolution at increasing evacuation temperatures are shown in Fig. 6. Bands at 1634 and 1461 cm^{-1}, due to physisorbed propylene, are only observed in the 25–100 °C temperature interval. Moreover, a shoulder at 1575 cm^{-1} starts to appear at a temperature of 150 °C, which is more evident at 200 and 250 °C. In addition to this, the band at 1461 increase in intensity and a new broad band in the 1683–1708 cm^{-1} interval are observed. The presence of the band at 1575 cm^{-1}, together with the band at 1461 cm^{-1}, could be related to the formation of acetate species, while the bands at 1683 cm^{-1} could be attributed to adsorbed acetone. As shown in Fig. 6 the formation of acetate species starts at some higher temperature than in the VAl-1 sample, and shows a lower intensity of the IR band. In this way, K-doped VO_x/Al_2O_3 sample seems to be less active in the transformation of C_3- and C_4-olefins than that of the VO_x/Al_2O_3 sample [10–12].

3.4.3. Adsorption of propylene on MoVNbO catalyst

The IR spectra of the MoVNb-3 sample after propylene adsorption at room temperature, and their evolution at several evacuation temperatures are shown in Fig. 7. Adsorption of propylene at rt leads to the formation of a strong band at 1607 cm^{-1} together with other less intense bands at 1436, 1376, and 1095 cm^{-1} (Fig. 7, spectrum a). The 1607 cm^{-1} band can be assigned to propylene π-bonded to a Lewis acid site, the 1436 and 1376 cm^{-1} IR bands correspond to the asymmetric and symmetric CH_3 deformations, while the band at 1095 cm^{-1} is due to isopropoxide species [45]. Increasing the temperature to 100 °C, a new band at 1672 cm^{-1} appeared, due to adsorbed acetone. In addition, an increase of the absorption bands at 1543 and 1434 cm^{-1} is also observed, while the band at 1095 cm^{-1}, related to isopropoxide compounds, disappears. From these results, it can be inferred the formation of acetate (bands at 1543 and 1434 cm^{-1}) as well as acetone (band at 1672 cm^{-1}) [47], in which isopropoxide can be proposed as intermediate species.

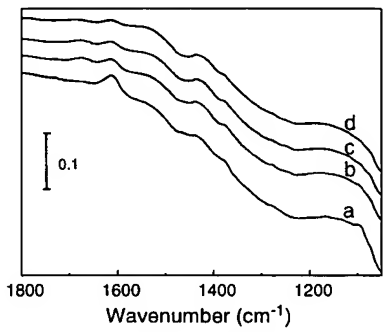

Fig. 7. FT-IR spectra of propylene adsorbed on MoVNb-3 sample at 25 °C (a); 100 °C (b); 150 °C (c); and 200 °C (d). Without reference spectra subtraction.

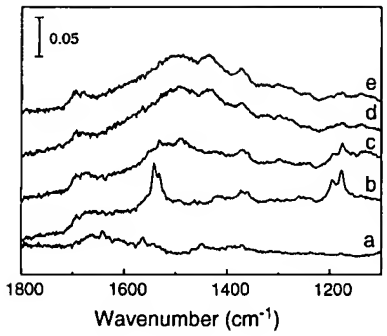

Fig. 8. FT-IR spectra of propylene adsorbed on MoVSb-4 sample at 25 °C (a); 100 °C (b); 150 °C (c); 200 °C (d) and 250 °C (e).

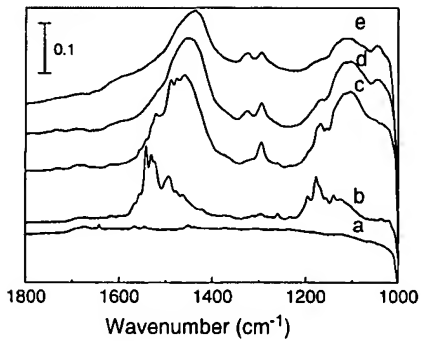

Fig. 9. FT-IR spectra of propylene adsorbed on MoVTeNb-5 sample at 25 °C (a); 100 °C (b); 150 °C (c); 200 °C (d) and 250 °C (e).

3.4.4. Adsorption of propylene on MoVSbO catalyst

IR spectra of the MoVSb-4 sample after propylene adsorption and their evolution with the evacuation temperature is shown in Fig. 8. The IR spectrum of propylene adsorbed after evacuation at room temperature is characterized by the presence of very weak bands at 1640, 1447 and 1368 cm^{-1}, which can be related to adsorbed unreacted propylene.

Increasing the temperature to 100 °C, the IR spectrum is characterized by the presence of very sharp bands at 1542, 1531 cm^{-1} together with bands at 1195 and 1177 cm^{-1} (Fig. 8, spectrum b). These bands can be assigned to enolic type compounds (C=C–O–) [39]. Other less intense bands at 1418, 1376 and 1359 cm^{-1} are also observed which could be related to δ_{CH_3} vibrations [48].

A decrease of the intensity of the sharp bands related to the enolic compound is observed by increasing the temperature up to 150 °C. This is clearly observed in the 1195–1175 cm^{-1} region where the C–O stretching vibration of the enolate compounds appeared. In addition, broad bands at 1540 and 1487 cm^{-1} arise, which are characteristic of acetate type compounds [45,46]. According to these results, enolic type compounds are mainly formed at 100 °C on the MoVSb-4 catalyst surface, which are precursor for the formation of acetate type compounds. Further increasing the temperature lead to a complete disappearance of bands related to enolate compounds and an increase of the intensity of bands due to acetate surface species (Fig. 8, spectra d and e).

3.4.5. Adsorption of propylene on MoVTeNbO catalyst

Fig. 9 shows the IR spectra of the MoVTeNb-5 catalyst after propylene adsorption at room temperature and their evolution with the evacuation temperature. The adsorption of propylene at room temperature leads to the appearance of weak bands at 1641, 1446 and 1367 cm^{-1}, related to physisorbed unreacted propylene. No isopropoxide type compounds have been observed (Fig. 9, spectrum a). The bands due to physisorbed propylene disappear by increasing the temperature at 100 °C, while new very intense bands at 1541, 1530, 1522, 1493 and 1195, 1177, 1169 cm^{-1} appear (Fig. 9, spectrum b). The bands at 1541, 1530, and 1195, 1177 cm^{-1}, also observed in the MoVSb-4 sample (Fig. 8, spectrum b), together to the presence of bands at 1522 and 1169 cm^{-1} can be attributed to different enolic compounds interacting with different sites on the catalyst surface. In addition to these, a new surface species characterized by a band at 1493 cm^{-1} is observed in the MoVTeNb-5 sample, which are not observed on the MoVSb-4 sample. The nature of this band has been revealed from time dependent adsorption experiments. IR spectra recorded in the first minutes after propylene adsorption at 100 °C reveal the presence of the band at 1493 cm^{-1} while no band in the 1190–1090 cm^{-1} IR region, associated to C–O stretching vibrations, is observed. Afterwards bands due to enolic compounds start to appear. Thus, and in agreement to other authors [43,49], the band at 1493 cm^{-1} is indicative of the formation of a π-allylic compound. Allylic species could be formed by a heterolytic dissociation of the C–H bond in the alkene CH_3 group.

At 150 °C the intensity of the bands due to enolic compounds decreases, which is clearly seen from the decrease in intensity of the bands in the 1195–1169 cm^{-1} IR region (Fig. 9, spectrum c). The evolution of the band at 1493 cm^{-1} cannot be easily followed since it is overlapped with strong broad bands at 1490 and 1440 cm^{-1}, characteristic of carboxilate compounds ($\nu_{as}COO$ and $\nu_{s}COO$, respectively) [48]. In fact these bands together with the band at 1294 cm^{-1} have been assigned to acrylate type compounds [47]. Thus, according to our results, π-allylic compounds are the precursors in the formation of acrylate compounds. It is interesting to indicate that the bands at 1493 cm^{-1} (at 100 °C) and 1294 cm^{-1} (at 150 °C) (related to π-allylic compounds and acrylate species, respectively) have not been observed in the MoVSb-4 sample.

Moreover, enolate type compounds are observed in both MoVSb-4 and MoVTeNb-5 samples, which in accordance to Figs. 8 and 9 have been attributed as precursors to the formation of acetate type compounds. However, the transformation of enolate type compounds into acetate compounds on MoVTeNb-5 sample should be low and will also be obscured due to the overlapping intense IR bands of acrylate compounds.

4. Discussion

4.1. Propane reaction network and nature of reaction intermediates

A common feature of the five catalysts is the formation of propylene at low propane conversions with initial selectivities to propylene of 35% (VAl-1), 40% (KVAl-2), 50% (MoVNb-3), 60% (MoVSb-4) and 90% (MoVTeNb-5). However, the selectivity to propylene decreases with the propane conversion with the appearance of other partial oxidation products: acrylic acid is mainly observed in sample MoVTeNb-5, while acetic acid is observed on sample MoVNb-3, and both acetic acid and acrylic acid in sample MoVSb-4. On the other hand, no oxygenated products other than carbon oxides were observed during the oxidation of propane on undoped and K-doped VO_x/Al_2O_3 catalysts, although the selectivity to propylene on K-doped catalyst (KVAl-2) was higher than that of the undoped VO_x/Al_2O_3 (VAl-1), which is in agreement to previous results on alkali-doped supported molybdenum or vanadium catalysts [10–12,35,50–53].

Accordingly, it can be concluded that propylene is directly formed from propane at low propane conversions and it is transformed to partial oxygenated products and/or carbon oxides at higher propane conversions on bulk mixed metal oxides (Scheme 1). So, propylene can be considered as a primary and unstable product during the oxidation of propane, while acrylic and acetic acids can be considered as secondary products. Moreover, carbon oxides are formed by both parallel and consecutive reactions (primary and secondary products), in agreement to previous results obtained on V-containing catalysts [1–5,26,27,33].

There is a parallelism between the reaction products observed from propane and propylene confirming that propylene is initially formed from propane. In addition, the catalytic results on propylene oxidation and the FT-IR spectra of propylene adsorbed show evidence that more than one pathway exists in these catalysts, although the importance of each mechanism depends on the characteristics of the catalysts. Scheme 2 summarizes the nature of adsorbed intermediates detected by IR after the adsorption of propylene on our catalysts: (i) a π-allylic intermediate, which is transformed into acrylic acid by a redox mechanism; (ii) an enolic type compound formed in the presence of Brønsted acid sites, which is transformed into acetone and then into acetic acid; (iii) a π-bonded propylene species interacting with Lewis acid sites, which in the presence of Brønsted acid sites lead to the formation of isopropoxide intermediates which can be proposed as precursor of carbon oxides.

Undoped and K-doped catalysts are moderately selective to propylene during the oxidation of propane, while CO_x are only observed during the oxidation of propylene. The incorporation of potassium increases the selectivity to propylene from propane (Fig. 1) but decreases the catalytic activity in both propane (Table 2) and propylene oxidation (Table 3). This agrees with the observation of Martín and Rives [35] that doping supported vanadia catalysts with sodium, leading a less acidic surface, enhances the selectivity to acrolein from propylene. IR spectra show the formation of π-bonded propylene species interacting with Lewis acid sites in both cases, although a lower oxidizing ability of the KVAl-2 sample toward the formation of acetate compounds is observed. Isopropoxide intermediate species formed in the presence of Brønsted acid sites of

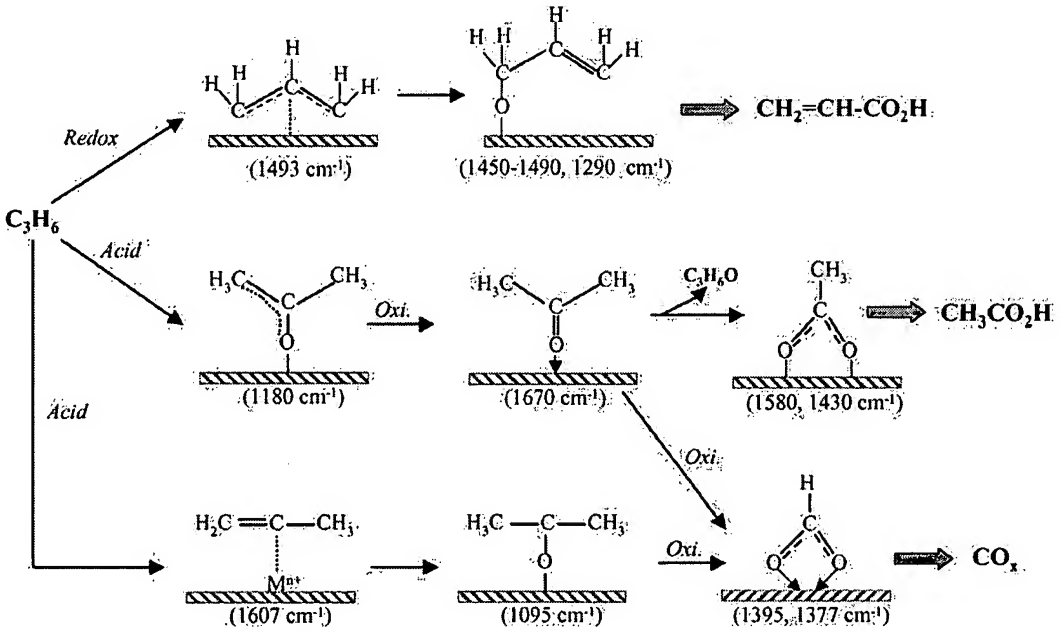

Scheme 2. Reaction intermediates observed in the adsorption/desorption of propylene over mixed metal oxides.

the Al_2O_3 support are not observed due to the high oxidizing ability of the VAl-1 sample. Acetate and formate compounds, formed by C–C cleavage of the adsorbed isopropoxide species by increasing temperature, are the precursors for the CO_x formation. So, the presence of Lewis and Brønsted acid sites in the undoped VAl-1 sample favours the consecutive deep oxidation of propylene during propane oxidation, but they are reduced if potassium is incorporated on the surface of the catalyst as occurs in KVAl-2 sample.

A different catalytic behaviour is observed in bulk catalysts during the oxidation of propane and propylene. Acetic acid is obtained on MoVNb-3, acrylic acid is selectively formed on MoVTeNb-5, and both acetic and acrylic acid are observed on MoVSb-4. The presence of Mo=O sites could partially explain the formation of partial oxidation products. However, the presence of α-hydrogen abstracting sites (Te^{4+} or Sb^{3+}) and/or the acid character of catalysts also determine the nature of these partial oxidation products. In this way, the formation of acetic acid on MoVTeNb-5 sample (with low selectivity) can be explained by the presence of a low amount of acid sites in this catalyst, confirming the importance of acid sites in non-desidered consecutive reactions.

Acrylic acid is formed from propylene by an allylic mechanism [1–5,26,27]. This is carried out by the α-hydrogen abstraction forming a symmetric π-allylic intermediate. Subsequently, the allylic intermediate reacts with lattice oxygen forming acrolein and acrylic acid. So, an active and selective catalyst for propylene requires an α-hydrogen-abstracting site, an O-insertion site, a redox component and a solid state matrix in which the key components can be intimately mixed [5,54–56]. Te^{4+}–O- [5,54,55] or Sb^{3+}–O-groups [5,56] have been proposed as responsible of the α-H abstraction of chemisorbed propylene in selective catalysts for partial oxidation of propylene, while Mo^{6+} sites have been proposed as the selective sites in the O-insertion into the π-allylic intermediate [1,2,56,57]. Accordingly, the formation of acrylic acid from propane or propylene on both MoVSb-4 and MoVTeNb-5 catalysts could be explained by the selective oxidation of propylene by an allylic mechanism, in which Sb^{3+} and Te^{4+}, respectively, are the α-hydrogen-abstracting sites and Mo^{6+} sites are the O-insertion ones. The absence of α-hydrogen-abstracting sites in the MoVNb-3 catalyst could explain the no formation of acrylic acid on this catalyst.

On the other hand, it is known that the presence of acid sites favours the formation of acetone and acetic acid from propylene [2,58]. In this way, V–Mo–O [58] mixed metal oxides, V_2O_5 [44] or VPO [44] catalysts are active and selective in the oxidative scission of propylene, in the presence of water vapour, to form acetone/acetic acid. In these cases, acetic acid could be formed by consecutive oxidation of the acetone formed at higher temperature [58]. Thus, the oxidative scission of propylene to acetic acid seems to comprise acetone formation, via the oxyhydration scission of the produced acetone to equimolecular acetic acid [44,58]. This mechanism is in good agreement to the IR spectra of propylene adsorbed on MoVNb-3 and MoVSb-4 catalysts (Figs. 7 and 8). In both cases acetate and/or acetone compounds are observed at a temperature of 150 °C after propylene adsorption. However the reaction intermediate is slightly different. In the first case π-bonded propylene interacting to Lewis acid sites are formed, while in the second case, enolate type compounds are mainly formed. This differences in the activation of the olefin could be related to the presence of V^{5+} and of more reduced Mo species in the MoVNb-3 sample as observed from XPS and FT-IR-NH_3 spectra.

According to the experiment of ammonia adsorbed on our catalysts (Fig. 4), it can be concluded that both MoVNb-3 and MoVSb-4 catalysts present the highest number of Lewis and Brønsted acid sites, which should be the active sites in the formation of acetic acid from propane and/or propylene. In this way, it has been reported that the incorporation of small amounts of potassium on the surface of a MoVSbO catalysts provokes the elimination of acid sites and the selective formation of acrylic acid rather than acetic acid, which is selectively observed in the K-free MoVSbO catalysts [33]. However, VAl-1 catalyst (with both Lewis and Brønsted acid sites) is not effective in the formation of acetic acid leading to the formation of carbon oxides. This may suggest that both the presence of Mo–O–V pairs, in addition to acid sites, are required in the transformation of propylene to acetone and/or acetic acid.

4.2. Nature of active sites in the selective and non-selective oxidation of propane

Since propylene is the main partial reaction product at low propane conversion (primary and unstable product, Fig. 1), a similar mechanism in the propane activation should be proposed in all cases). In this way, it is generally accepted that the oxidative dehydrogenation of propane to propylene is the first step in the selective (amm)oxidation of propane to acrylonitrile and acrylic acid on Mo–V–Te–Nb–O [18–27] and Mo–V–Sb–O [30–33] catalysts. This oxidative activation of propane should be initiated via H-abstraction from propane by concerted mechanism over acid–base pairs: the Lewis acid site (V^{5+} cation) and the basic oxygen (O^{2-}) interacting with the α- and β-hydrogen of propane, respectively, to form propylene [1–5,59].

Tetrahedral V^{5+} species are mainly observed in the undoped and K-doped catalysts [11,12], which are, in agreement to previous results, the active and relatively selective species for the oxidative dehydrogenation of short chain alkanes [6–12]. However, as it has been discussed previously [10–12,35,50–54], the different acid–base character of these catalysts determine the final selectivity to the olefin.

Octahedral V^{5+} species in V–O–Mo^{n+} pairs can be proposed as the active species in the oxidative activation of propane over bulk Mo–V-based catalysts [1,5,13–33]. However, the presence of other active sites for propylene oxidation favours the

formation of partial oxidation products. Thus, the presence of Mo^{6+} sites in addition to Te^{4+} or Sb^{3+} sites could favour the formation of partial oxygenated products by a consecutive oxidation of propylene [1–5,24,55,56,60]. Since both MoVSbO and MoVTeNbO catalysts present similar crystalline phases, the different reaction products observed over these bulk catalysts should be related to their chemical compositions. In this way, Mo^{6+} seems to be involved in both the adsorption of propylene and in the O-insertion in partial oxygenated products [33]: (i) to form acrylic acid, when α-hydrogen-abstracting sites (i.e. Sb^{3+} or Te^{4+}) are present; and/or (ii) to form acetic acid, when Lewis and/or Brønsted acid sites are present in the catalysts. The presence of Brønsted acid sites has a negative effect on the selective oxidation of propane to acrylic acid since they favour the parallel formation of acetone/acetic acid in Mo-containing catalysts or the deep oxidation of propylene in Mo-free catalysts. Thus, the results obtained on MoVSb-4 catalyst can be explained by the competition between the allylic oxidation and the oxidative scission of propylene intermediate by the presence of Brønsted acid sites. However, the incorporation of potassium on the catalyst surface, i.e. K-promoted MoVSbO catalysts [33], eliminate the acid sites favouring the selective formation of acrylic acid. This was also observed during the oxidation of propane on Te-doped VPO, in which the incorporation of Te decreases the number of acid sites favouring the formation of allylic compounds, i.e. acrolein and acrylic acid [44].

The results presented here show the key factors of a selective catalyst in the oxidation of propane to acrylic as MoVTeNbO catalyst. It should present an alkane activation site (V^{5+}-sites), an α-hydrogen-abstracting site (Te^{4+}) and an O-insertion site (Mo^{6+}) in a well defined structure, i.e. $Te_2M_{20}O_{57}$ (M = Mo, V, Nb) [5,22,24,28,60]. This is also observed during the adsorption experiments with propylene. On the other hand, a selective catalyst should present a small number of acid sites (both Lewis and Brønsted) in order to decrease the formation of acetic acid from propylene by a hydration mechanism. These results explain how Mo–V–Te–Nb mixed metal oxides catalysts are active and very selective in the oxidation of propane and propylene to acrylic acid. As a difference with the MoVSbO catalyst, the incorporation of Te^{4+} atoms rather than Sb^{3+} sites in a well defined structure can be responsible of the lower number of acid sites and the lower formation of acetic acid on MoVTeNbO catalysts. Thus, as suggested in K-promoted MoVSbO catalysts [33], the nature and strength of acid sites should be tailored in order to optimise allylic oxidation and to avoid oxidative breaking of C–C bonds.

5. Conclusions

In conclusion, a series of V-based catalysts, i.e. supported (undoped and K-doped VO_x/Al_2O_3) and bulk (MoVNb-, MoVSb- and MoVTeNb-oxide) catalysts, have been tested in the oxidation of propane and propylene and the results compared with those obtained by FT-IR of preadsorbed propylene or NH_3. In all cases, propylene is directly formed from propane suggesting that V species are involved in the oxidative activation of propane. However, different reaction products are observed at high propane conversions, as a consequence of the different propylene oxidation on each catalyst: (i) acrylic acid on MoVTeNb-oxide catalysts; (ii) Both acetic acid and acrylic acid on MoVSb-oxide catalysts; (iii) acetic acid formed on MoVNb-oxide catalyst; and (iv) CO and CO_2 mainly observed on undoped and K-doped VO_x/Al_2O_3.

The presence of Mo-sites seems to be important in the formation of partial oxidation products from propylene, but the ratio between allylic oxidation (i.e. acrylic acid) and oxidative scission (i.e. acetic acid) can be related to the number and strength of acid sites in the catalyst. According to the nature of the catalyst, different reaction intermediates are observed by FT-IR of propylene adsorbed on these catalysts, i.e. π-allylic compounds and enolate compounds, which are the precursors in the formation of acrylic acid and acetic acid, respectively. In addition to these, the presence of π-bonded propylene species interacting with Lewis acid sites, as occurs in supported vanadia catalysts, are also observed. These π-bonded propylene species, in the presence of Brønsted acid sites, lead to the formation of isopropoxide species which can be proposed as the precursors of carbon oxides.

The comparison of the behaviour of these catalysts toward propane and propylene oxidation, propylene adsorption and ammonia adsorption shows evidence of the different reactivity of their surface sites, and suggest the key factors of a selective catalyst in the oxidation of propane to acrylic acid. Thus, and in addition to the presence of an alkane activation site (V^{5+}-sites), an α-hydrogen-abstracting site (Te^{4+} or Sb^{3+}) and an O-insertion site (Mo^{6+}) in a well defined host structure, i.e. $Te_2M_{20}O_{57}$ (with M = Mo, V, Nb) or $Sb_2M_{10}O_{31}$ (with M = Mo, V), the selective catalysts for propane oxidation to acrylic acid should have a relatively low number of Brønsted acid sites. In fact, the presence of Brønsted acid sites in Mo- and V-containing catalysts, as occurs in MoVSbO or MoVNbO mixed metal oxide, favours the formation of acetic acid (by an oxidative scission mechanism) rather than acrylic acid (by an allylic mechanism), while the formation of acetic acid in selective MoVTeNbO catalysts is generally very low.

Acknowledgment

Financial support from DGICYT in Spain through Projects PPQ2003-03946 is gratefully acknowledged.

References

[1] S. Albonetti, F. Cavani, F. Trifiró, Catal. Rev.-Sci. Eng. 38 (1996) 413.

[2] M.M. Bettahar, G. Costentin, L. Savary, J.C. Lavalley, Appl. Catal. A: Gen. 145 (1996) 1.
[3] M.M. Lin, Appl. Catal. A: Gen. 207 (2001) 1.
[4] T. Ushikubo, Catal. Today 78 (2003) 79.
[5] R.K. Grasselli, J.D. Burrington, D.J. Buttrey, P. DeSanto, C.G. Lungmair, A.F. Volpe, T. Weingand, Top. Catal. 23 (2003) 5.
[6] T. Blasco, J.M. López Nieto, Appl. Catal. A: Gen. 157 (1997) 117.
[7] E.A. Mamedov, V. Cortés-Corberán, Appl. Catal. A: Gen. 127 (1995) 1.
[8] F. Cavani, F. Trifiró, Catal. Today 24 (1995) 307.
[9] H.H. Kung, Adv. Catal. 40 (1994) 1.
[10] J.M. López Nieto, R. Coenrads, A. Dejoz, M.I. Vázquez, Stud. Surf. Sci. Catal. 110 (1997) 767.
[11] A. Galli, J.M. López Nieto, A. Dejoz, M.I. Vázquez, Catal. Lett. 34 (1995) 51.
[12] P. Concepción, S. Kuba, H. Knözinger, B. Solsona, J.M. López Nieto, Stud. Surf. Sci. Catal. 130 (2000) 767.
[13] E.M. Thorsteinson, T.P. Wilson, F.G. Young, P.H. Kasai, J. Catal. 52 (1978) 116.
[14] M. Merzouki, B. Taouk, L. Monceaux, E. Bordes, P. Courtine, Stud. Surf. Sci. Catal. 72 (1992) 165.
[15] D. Linke, D. Wolf, M. Baerns, O. Timpe, R. Schogl, S. Zeyβ, U. Dingerdisen, J. Catal. 205 (2002) 16.
[16] P. Botella, J.M. López Nieto, A. Dejoz, M.I. Vázquez, A. Martínez-Arias, Catal. Today 78 (2003) 507.
[17] A.A. Adesina, N.W. Cant, A. Saberi-Mghaddam, C.H. Szeto, D. Trimm, J. Chem. Technol. Biotecnol. 72 (1998) 19.
[18] Z. Zhao, X. Gao, I.E. Wachs, J. Phys. Chem. B 107 (2003) 6333.
[19] T. Ushikubo, K. Oshima, A. Kayo, T. Umezawa, K. Kiyono, I. Sawaki, EP Patent 529853 A2 (1992).
[20] T. Ushikubo, K. Oshima, A. Kayou, M. Hatano, Stud. Surf. Sci. Catal. 112 (1997) 473.
[21] H. Watanabe, Y. Koyasu, Appl. Catal. A: Gen. 194/195 (2000) 479.
[22] J.M.M. Millet, H. Roussel, A. Pigamo, J.L. Dubois, J.C. Jumas, Appl. Catal. A: Gen. 232 (2002) 77.
[23] H. Tsuji, Y.J. Koyasu, J. Am. Chem. Soc. 124 (2002) 5608.
[24] P. DeSanto, D.J. Buttrey, R.K. Grasselli, C.G. Lugmair, A.F. Volpe, B.H. Toby, T. Vogt, Top. Catal. 23 (2003) 23.
[25] T. Ushikubo, H. Nakamura, Y. Koyasu, S. Wajiki, US Patent 5 380 933 (1995).
[26] P. Botella, J.M. López Nieto, A. Martínez-Arias, B. Solsona, Catal. Lett. 74 (2001) 149.
[27] L. Luo, J.A. Labinger, M.E. Davis, J. Catal. 200 (2001) 222.
[28] P. Botella, E. García-Gonzalez, J.M. López Nieto, A. Dejoz, M.I. Vázquez, J. González-Calbet, J. Catal. 225 (2004) 428.
[29] (a) J.M. López Nieto, P. Botella, M.I. Vázquez, A. Dejoz, Chem. Commun. (2002) 1906;
(b) J.M. López Nieto, P. Botella, M.I. Vázquez, A. Dejoz, WO Patent 0 364 035 (2003).
[30] H. Hinago, K. Hiroyuki, DE Patent 10145958 A1 (2001).
[31] J.C. Vedrine, E.M. Novakova, E.G. Derouane, Catal. Today 81 (2003) 27.
[32] J.M.M. Millet, M. Baca, A. Pigamo, D. Vitry, W. Ueda, J.L. Dubois, Appl. Catal. A: Gen. 244 (2003) 359.
[33] P. Botella, P. Concepción, J.M. López Nieto, B. Solsona, Catal. Lett. 89 (2003) 249.
[34] C.D. Wagner, L.E. Davis, M.V. Séller, J.A. Taylor, R.H. Raymond, L.H. Gale, Surf. Interf. Anal. 13 (1981) 211.
[35] C. Martín, V. Rives, J. Mol. Catal. 48 (1988) 381.
[36] M. Parmentier, G. Gleitzer, R.J.D. Tilley, J. Solid State Chem. 31 (1989) 305.
[37] M. Lundberg, M. Sundberg, Ultramicroscopy 52 (1993) 429.
[38] G. Mestl, Ch. Linsmeier, R. Gottschall, M. Dieterle, J. Find, D. Herein, M. Jäger, Y. Uchida, R. Schlögl, J. Mol. Catal. A 162 (2000) 463.
[39] A. Andersson, S.L.T. Andersson, G. Centi, R.K. Graselli, M. Sanati, F. Trifiró, Appl. Catal. A: Gen. 113 (1994) 43.
[40] S. Damyanova, L. Petrov, M.A. Centeno, P. Grange, Appl. Catal. A: Gen. 224 (2002) 271.
[41] J.M. Aigler, V.B. Kazansky, M. Huolla, A. Proctor, D.M. Hercules, J. Phys. Chem. 99 (1995) 11489.
[42] H. Knoezinger, NATO ASI Ser. C: Math. Phys. Sci. 398 (1993) 267.
[43] A.A. Davydov, in: C.H. Rochester (Ed.), Infrared Spectroscopy of Adsorbed Species on the Surface of Transition Metal Oxides, John Wiley & Sons, 1990.
[44] M. Ai, J. Catal. 101 (1986) 473.
[45] V. Ermini, E. Finocchio, S. Sechi, G. Busca, S. Rossini, Appl. Catal. A: Gen. 190 (2000) 157.
[46] E. Heraclous, A.A. Lemonidou, J.A. Lercher, Appl. Catal. A: Gen. 264 (2004) 73.
[47] V.S. Sanchez Escribano, G. Busca, V. Lorenzelli, J. Phys. Chem. 94 (1990) 8939.
[48] V.A. Matyshak, O.V. Krylov, Catal. Today 25 (1995) 1, and references therein.
[49] A.A. Davydov, V.G. Mikhaltchenko, V.D. Sokolovskii, G.K. Boreskov, J. Catal. 55 (1978) 299.
[50] B. Grzybowska-Swierkosz, Top. Catal. 21 (2002) 35, and references therein.
[51] J.C. Vedrine, Top. Catal. 21 (2002) 97.
[52] R.B. Watson, U.S. Ozkan, J. Catal. 191 (2000) 12.
[53] K. Chen, S. Xie, A.T. Bell, E. Iglesia, J. Catal. 195 (2000) 244.
[54] J.C.J. Bart, N. Giordano, J. Catal. 64 (1980) 356.
[55] R.K. Grasselli, G. Centi, F. Trifiró, Appl. Catal. 57 (1990) 149.
[56] J.D. Burrington, C.T. Kartisek, R.K. Grasselli, J. Catal. 87 (1984) 363.
[57] Y.H. Jang, W.A. Goddard, J. Phys. Chem. B 106 (2002) 5997.
[58] T. Seiyama, K. Nita, T. Mahehara, N. Yamazoe, Y. Takita, J. Catal. 49 (1977) 164.
[59] T. Sishido, T. Konishi, I. Matsuura, Y. Wang, K. Takaki, K. Takehira, Catal. Today 77 (2001) 77.
[60] P. Botella, J.M. López Nieto, B. Solsona, A. Mifsud, F. Márquez, J. Catal. 209 (2002) 445.

Available online at www.sciencedirect.com
SCIENCE DIRECT
Journal of Catalysis 228 (2004) 362–373
JOURNAL OF CATALYSIS
www.elsevier.com/locate/jcat

Selective oxidation of propane to acrylic acid on K-doped MoVSbO catalysts: catalyst characterization and catalytic performance

T. Blasco [a], P. Botella [a], P. Concepción [a], J.M. López Nieto [a,*], A. Martinez-Arias [b], C. Prieto [c]

[a] *Instituto de Tecnología Química, UPV-CSIC, Avenida de los Naranjos s/n, 46022-Valencia, Spain*
[b] *Instituto de Catálisis y Petroleoquímica, Campus UAM Cantoblanco, 28049 Madrid, Spain*
[c] *Instituto de Ciencia de Materiales, CSIC, Cantoblanco, 28049 Madrid, Spain*

Received 22 June 2004; revised 23 August 2004; accepted 31 August 2004

Available online 28 October 2004

Abstract

K-doped Mo–V–Sb mixed oxides catalysts have been prepared by impregnation of a MoVSbO mixed oxide (previously prepared by hydrothermal synthesis) with an aqueous solution of potassium nitrate, characterized by XRD, SEM-EDX, EPR, XPS, XANES, and FTIR of adsorbed NH_3, and tested in the selective oxidation of propane and propylene in the 593–693 K temperature range. The undoped MoVSbO catalysts presented a selectivity to acrylic acid lower than 15%, while selectivities to acrylic acid of about 40% can be obtained on K-doped catalysts. No appreciable differences between undoped and K-doped catalysts are observed in the nature of crystalline phases present in each case, on the basis of X-ray diffraction analysis. However, important differences in both the oxidation state of surface Sb species (according to XPS evidence) and the number of acid sites (determined from FTIR of adsorbed NH_3) are observed between the undoped and the K-doped catalysts. The high selectivity to acrylic acid on the K-doped catalysts seems to be related to changes in the acid–base properties of the catalysts and most particularly to the elimination of (Brønsted) acid sites. In addition, the role of antimony species in activity and selectivity is also discussed and a reaction network for the partial oxidation reaction is proposed.

Keywords: Selective oxidation of propane to acrylic acid or acetic acid; K-doped Mo–V–Sb mixed metal oxide catalyst; Hydrothermal synthesis; Catalyst characterization (X-ray diffraction, XANES, EPR, XPS, FTIR of adsorbed ammonia)

1. Introduction

There is an increasing interest in the development of a process for direct oxidation of propane to acrylic acid as an alternative to the two-step conventional industrial process based on the propylene feedstock, which represents approximately 90% of the 1.84×10^6 tons/year of the total capacity of acrylic acid production plants [1,2]. Although a large number of catalytic systems have been studied, only few catalysts seem to be relatively active and selective [3,4]. This is the case of undoped and Me-doped V–P–O oxides [5–7], Ni–Mo–Te–P–O oxides [8,9], and metal and/or pyridine exchanged molybdovanadophosphoric acid [1–14].

MoVNbTe(Sb) catalysts have been recently proposed as active and selective in the oxidation of propane to acrylic acid [15–24], but the selectivities achieved on Sb-containing catalysts [19–23] are generally lower than those obtained on Te-containing catalysts [15–18]. Despite their practical interest, few fundamental studies on the nature and catalytic behavior of MoVSb-based catalysts have been published [20–23]. Although some factors seem to have an important influence on the selectivity to acrylic acid, such as the catalyst calcination conditions [20,21] or the incorporation of water in the feed [22], relatively low selectivities to acrylic acid have been reported.

Characterization results published on MoVSbO [23] and MoVSbNbO [20,21] catalysts suggest the presence of several crystalline phases depending on the chemical composition, the catalyst preparation procedure, and the calcina-

* Corresponding author. Fax: +34 96 3877809.
E-mail address: jmlopez@itq.upv.es (J.M. López Nieto).

0021-9517/$ – see front matter
doi:10.1016/j.jcat.2004.08.036

tion conditions. $Sb_4Mo_{10}O_{30}$ and $Sb_2Mo_{10}O_{31}$ in addition to $Mo_{5-x}(V/Nb)_xO_{14}$ were proposed to be present on samples prepared by a slurry method and heat-treated at 873 K in N_2 and activated in He or in O_2/He mixtures (20% of O_2), although some changes in the DRX were observed depending on the activation procedure [20,21]. $(Sb_2O)M_6O_{18}$ and $(SbO)_2M_{20}O_{56}$ (with M = Mo and V) were proposed, however, in MoVSbO catalysts prepared by hydrothermal synthesis and activated in air at 643 K for 20 min followed by a second heat treatment, in pure nitrogen, at 873 K for 2 h [26]. Nevertheless, the similarities of the XRD patterns of the oxides involved and the complexity of the systems render difficult an unambiguous interpretation of the diffraction data, and to get additional information, which may help to elucidate the crystallographic phases, present, by using other characterization techniques. In this sense, one of the differences among these crystalline phases is the Sb oxidation state, which is Sb^{3+} in $Sb_4Mo_{10}O_{30}$ and $Sb_2Mo_{10}O_{31}$ [20,25] and Sb^{3+}/Sb^{5+} in $(Sb_2O)M_6O_{18}$ and $(SbO)_2M_{20}O_{56}$ [26].

MoVSbO catalysts, prepared by hydrothermal synthesis, have also been studied in the partial oxidation of propane [23]. They present a selectivity to acrylic acid (ca. 6%) lower than that obtained on Te-based catalysts [16,23, 24], although their catalytic performance has partially been enhanced by grinding the catalyst precursor before the calcination step. However, selectivities to acrylic acid lower than 20% have been reported [23].

Recently, it has been shown that the selectivity to acrylic acid obtained during the selective oxidation of propane on MoVSbO catalysts can be improved by the incorporation of potassium on the catalyst surface [27]. This higher production of acrylic acid could be related to the modifications of the nature and number of acid sites on the catalyst surface after the incorporation of potassium. However, the role of each element and the nature of the crystalline phases are still unclear.

In this paper we will present the characterization and catalytic behavior of undoped and K-doped MoVSbO, in which the incorporation of potassium has a promoter effect on the catalytic performance for the selective oxidation of propane to acrylic acid. The characterization results show no changes in the bulk of the catalysts after the incorporation of potassium, suggesting that the higher selectivity to acrylic acid observed on K-doped catalysts could be mainly related to the modification of both the number and the nature of acid sites rather than changes in the oxidation state of the Sb cations on the catalyst surface.

2. Experimental

2.1. Catalyst preparation

A Mo–V–Sb mixed metal oxide catalyst was prepared by a hydrothermal method, using vanadyl sulfate, antimony sulfate, ammonium heptamolybdate, and water with a Mo/V/Sb atomic ratio of 1/0.18/0.15. The gel was autoclaved in Teflon-lined stainless-steel autoclave at 448 K for 48 h. The resulting precursor was filtered, washed, dried at 353 K for 16 h, and heat-treated at 873 K for 2 h in N_2 stream. It will be called the **MVS** sample.

K-doped Mo–V–Sb mixed metal oxide catalysts (with K/Mo atomic ratios from 0.002 to 0.02) have been prepared by impregnation of the **MVS** sample with aqueous solutions of potassium nitrate. The samples were then rotavapored at 323 K and 14 kPa. The resulting powders were dried overnight at 373 K and finally heat-treated at 773 K for 1 h in a N_2 stream. The samples will be named **MVSK-*n*** (n = 1 to 4); their main characteristics are shown in Table 1.

For comparative purpose, a portion of the MVS precursor was first calcined in air at 553 K (2 h) and then heat-treated at 873 K (2 h) in N_2. This sample will be referred to as **MVS-A-N**.

2.2. Catalyst characterization

X-ray diffraction patterns (XRD) were collected using a Philips X'Pert diffractometer equipped with a graphite monochromator, operating at 40 kV and 45 mA and employing nickel-filtered Cu$K\alpha$ radiation (λ = 0.1542 nm).

Scanning electron microscopy (SEM) and EDX microanalyses were performed on a JEOL JSM 6300 LINK ISIS instrument. The quantitative EDX analysis was performed using an Oxford LINK ISIS System with the SEMQUANT program, which introduces the ZAF correction.

Infrared spectra of the samples diluted in KBr (20 mg of the sample mixed with 100 mg of dry KBr and pressed into a disk) were obtained with a Nicolet 710 FTIR spectrometer.

Electron paramagnetic resonance spectra (EPR) were recorded with a Bruker ER-200D spectrometer working in the X-band and calibrated with a DPPH standard (g = 2.0036). Quantitative analysis was carried out by double integration of the EPR spectra and comparison with a copper sulfate ($CuSO_4 \cdot 5H_2O$) standard. Computer simulations were employed to determine experimental parameters or to quantify contributions of overlapping signals. Portions of ca. 40 mg of sample were introduced inside an EPR quartz probe cell and subjected (under conventional high vacuum conditions) to extensive room temperature outgassing prior to recording their spectra.

Photoelectron spectra (XPS) were recorded on a VG-Escalab-210 Spectrometer using Al$K\alpha$ radiation (Al$K\alpha$ = 1486 eV) operated at 12 kV and 20 mA. The spectrometer's hemispherical analyzer was set to 50 eV constant pass energy. The samples were previously outgassed at 373 K for 2 h in the preparation chamber of the spectrometer and subsequently transferred to the analysis chamber where the pressure during spectra acquisition was 5×10^{-10} Torr. The binding energy (BE) data were referenced to C1s (BE = 284.5 eV) from surface contamination. Atomic ratios of the elements were calculated from the relative peak areas

Table 1
Characteristics of undoped and K-doped Mo–V–Sb–O catalysts

Catalyst	S_{BET}[a]	K/Mo atomic ratio[b]	Mo–V–Sb–K atomic ratio[b]	Mo–V–Sb–K surface atomic ratio[c]	EDX analysis	
					Particle number[d]	Composition
MVS	9.5	0	$Mo_1V_{0.18}Sb_{0.15}$	$Mo_1V_{0.19}$–$Sb_{0.08}$	1	$MoV_{0.30}Sb_{0.34}$
					2–3–4	$MoV_{0.29-0.33}Sb_{0.18-0.20}$
					5–6	$MoV_{0.13-0.20}Sb_{0.18-0.20}$
					7	$MoV_{0.07}Sb_{0.05}$
MVSK-1	nd	0.002	$Mo_1V_{0.18}Sb_{0.15}K_{0.002}$	nd	nd	
MVSK-2	6.8	0.005	$Mo_1V_{0.18}Sb_{0.15}K_{0.005}$	nd	1–2	$MoV_{0.29-0.32}Sb_{0.18-0.20}K_{0.006-0.008}$
					3	$MoV_{0.24-0.26}Sb_{0.08-0.12}K_{0.006-0.008}$
					4	$MoV_{0.08}Sb_{0.05}K_0$
MVSK-3	nd	0.010	$Mo_1V_{0.18}Sb_{0.15}K_{0.01}$	$Mo_1V_{0.20}Sb_{0.10}K_{0.015}$	nd	
MVSK-4	6.6	0.020	$Mo_1V_{0.18}Sb_{0.15}K_{0.02}$	$Mo_1V_{0.21}Sb_{0.11}K_{0.016}$	1	$MoV_{0.22}Sb_{0.34}K_{0.004}$
					2–3–4–5–6	$MoV_{0.25-0.33}Sb_{0.12-0.20}K_{0.01-0.03}$
MVS-A-N	nd	0	$Mo_1V_{0.18}Sb_{0.15}$	$Mo_1V_{0.22}Sb_{0.17}$	nd	

[a] S_{BET} in $m^2\ g^{-1}$; nd = not determined.
[b] Chemical analysis was obtained by atomic absorption spectroscopy of heat-treated samples.
[c] Mo–V–Sb–K surface atomic ratio was determined by XPS.
[d] Particle number in Fig. 3.

of the respective core-level lines using the Wagner sensitivity factors [28]. The influence of the Kα3,4 satellite of the O1s line has been taken into account for the integration of the V2p3/2 core-level line. Thus, the satellite subtraction (intensity ratios I/I_0 and energies distances ΔE, between main line and satellite) has been adjusted by using a reference material without vanadium in order to obtain a smooth background baseline, as indicated in Ref. [29]. By optimising the above mentioned parameters, the values obtained for the satellite subtraction are Kα3: $I/I_0 = 0.06225$, $\Delta E = 9.8$ eV; and Kα4: $I/I_0 = 0.030$, $\Delta E = 11.8$ eV. Determination of the O1s peak area is calculated after subtraction of the Sb3d5/2 peak area (assuming a 3:2 peak ratio of the 3d5/2:3d3/2 doublets). Data analysis procedures involve smoothing, a Shirley background subtraction, and curve fitting using mixed Gaussian–Lorentzian functions by a least-squares method.

Sb L_I edge XANES spectra were acquired at room temperature at the line D42, XAS 13 beamline, at the LURE Synchrotron Radiation facility (Orsay, Paris) using a double crystal Si (311) monochromator, detuned until 50%. Detection was made in the transmission mode by using two ion chambers with air filled gas. Three scans were collected for every spectra in the range 4650–4680 eV, with varying energy steps in three regions: 0.5 eV/s between 4650 and 4680 eV, 0.2 eV/s in the 4680–4735 eV region, and 0.4 eV/s in the range 4735–4780 eV. Linear background absorption was subtracted to the entire spectra, which was then normalized at approximately 50 eV above the absorption edge. The spectrum of $FeSbO_4$ was recorded as a reference for the position of the Sb^{5+} cation, with the absorption maximum at 4707.5 eV.

Infrared spectra of adsorbed ammonia were obtained in a Bio-Rad Fis-4017 spectrophotometer. Wafers of 10 mg cm^{-2}, mounted in a Pyrex vacuum cell fitted with KRS-5 windows, were degassed at 473 K for 2 h and then cooled at room temperature. Ammonia was first admitted at room temperature, degassed for 1 h, and finally desorbed at 298–373 K.

2.3. Catalytic tests

The catalytic experiments were carried out in a fixed-bed quartz tubular reactor (i.d. 20 mm, length 400 mm), working at atmospheric pressure [24]. Catalyst samples (0.3–0.5 mm particle size) were introduced in the reactor and diluted with 2–4 g of silicon carbide (0.5–0.75 mm particle size) in order to keep a constant volume in the catalyst bed. The feed consisted of a mixture of $C_3H_8/O_2/H_2O$/He or $C_3H_6/O_2/H_2O$/He molar ratio of 4/8/30/58 or 4/9/30/57, respectively. Experiments were carried out in the 613–673 K temperature interval in order to achieve the highest selectivity to partial oxidation products. Reactants and reaction products were analyzed by on-line gas chromatography [16]. Blank runs showed that the homogeneous reaction could be neglected under the experimental conditions used in this work.

3. Results

3.1. Catalyst characterization

A slight decrease of the surface area is observed upon the incorporation of potassium in the MoVSbO catalyst (Table 1), indicating that neither the incorporation of potassium by impregnation nor a second heat-treatment in N_2 at 773 K for 1 h have a strong influence on the specific surface area of MoVSb-based catalysts.

The XRD pattern of the undoped MoVSbO catalyst is shown in Fig. 1a. The appearance of peaks at $2\theta = 22.3$, 25.8, 28.3, 36.3, 45.0, and 50.0° can be attributed to the presence of a Sb^{3+}-containing compound like $Sb_4Mo_{10}O_{30}$

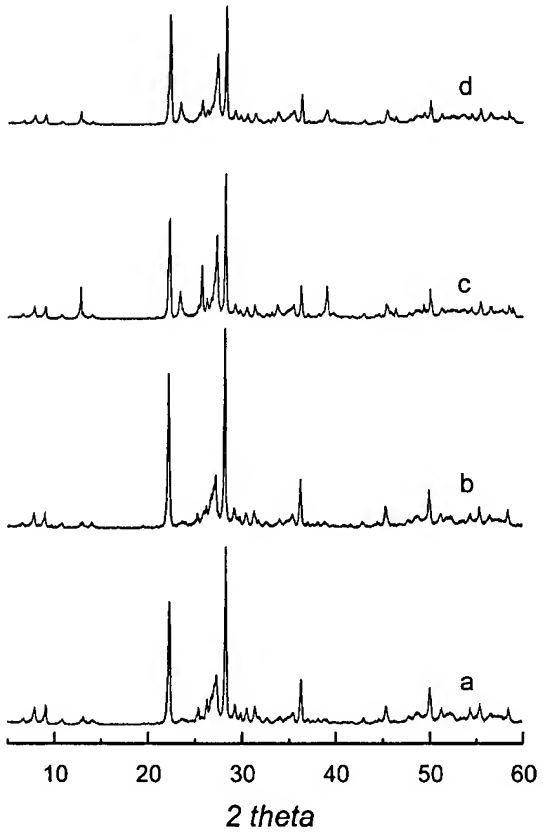

Fig. 1. XRD patterns of undoped and potassium-doped MoVSbO catalysts: (a) MVS; (b) MVSK-4; (c) MVS-A-N; (d) MVS-A-N after reaction test.

[JCPDS, 33-0104] [20,21], although the formation of $(Sb_2O)M_6O_{19}$ (with M = Mo and V), a Sb^{5+}/Sb^{3+}-containing crystalline phase [26] cannot be ruled out. Besides this, peaks at $2\theta = 6.6$, 7.8, 8.9, 22.3, 26.3, 26.7, 27.3, and 29.3° could be related to the presence of a Sb^{3+}-containing compound like $Sb_2Mo_{10}O_{31}$ [JCPDS: 33-105] [20,21], although the formation of $(SbO)_2M_{20}O_{56}$ (with M = Mo and V), a Sb^{5+}/Sb^{3+}-containing phase [26], $(V_{0.07}Mo_{0.93})_5O_{14}$ [JCPDS: 31-1437] should also be considered. No significant differences are appreciated in the XRD patterns when comparing undoped and K-doped MoVSbO samples (Fig. 1b), although changes in the proportion between $Sb_2Mo_{10}O_{31}/Sb_4Mo_{10}O_{30}$ or the presence of $(SbO)_2M_{20}O_{56}/(Sb_2O)M_6O_{18}$ cannot be detected by XRD. Furthermore, additional peaks at $2\theta = 12.9$, 25.4, 27.2, and 38.9° which can be due to the formation, as minor phases, of undoped or metal-doped MoO_3 [JCPDS: 5-508] are present in both the K-free and the K-doped samples. The intensity of these peaks is particularly high in the **MVS-A-N** sample (Fig. 1c). This suggests that, in this case, a partial oxidation of the catalyst is produced during the calcination in air at 553 K.

The morphology of the catalysts has been studied by scanning electron microscopy with X-ray energy dispersive analysis (EDX). The results obtained are collected in Table 1. The SEM image of the catalysts (not reported) shows

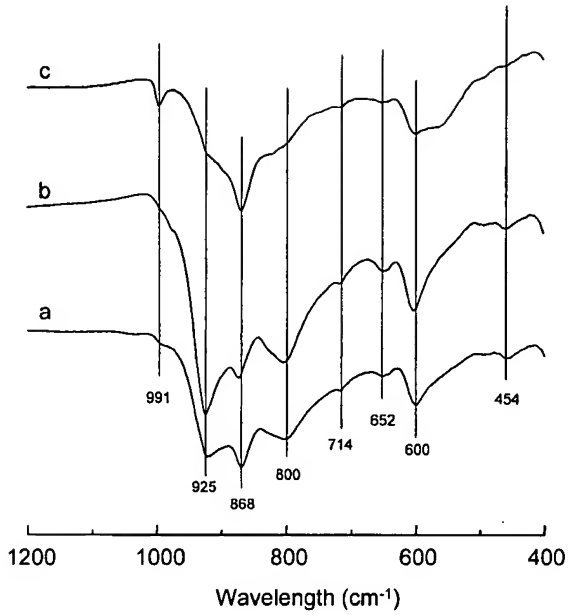

Fig. 2. IR spectra of undoped and K-doped catalysts: (a) **MVS**; (b) **MVSK-4**; (c) **MVS-A-N**.

the presence of agglomerates containing small slabs and rods of less than 5 μm in diameter. This morphology is similar to those previously observed in Te- [23,24] or Sb-based [23] catalysts prepared by hydrothermal synthesis. The global chemical composition obtained by EDX analysis is in fair agreement with those obtained by AAS (Table 1). Nevertheless, the SEM-EDX analysis evidences the presence of local inhomogeneities in the composition of the particles, with Sb-depleted zones, in some cases associated with lower V concentrations (Table 1). In every case, the composition of the crystals seems to be consistent with the crystalline phases observed by XRD.

Fig. 2 shows the IR spectra of undoped and K-doped catalysts. In agreement with the XRD results, the introduction of K in the Mo–V–Sb catalyst does not produce strong changes in the bulk of the catalyst, as no significant differences are found in the positions of the bands between samples with variable K content. The modifications observed in the overall or relative intensities of a determinate group of bands must rather be associated with K incorporation at surface positions. The bands at 868, 800, 714, and 652 cm^{-1} can be attributed to antisymmetric vibrations of Mo–O–Me (Me = Mo, Sb) bridging bonds [20,24,30]. The bands at ca. 925, 600, and 454 cm^{-1} are probably related to V=O groups and V–O–Me bonds (Me = Mo, V) [20,24,29] and/or to the presence of $Sb_2Mo_{10}O_{31}$ [20]. A shoulder at 990 cm^{-1} indicates the presence of Mo=O *cis*-dioxo groups of MoO_3 [30], which contribute to the band at 868 cm^{-1} too.

EPR spectra recorded at 77 K consist in all cases essentially in the overlapping of two signals. An example of spectrum deconvolution is shown in Fig. 3 for the **MVS** sample. All spectra basically consist in the overlapping of a major broad symmetric signal **A1** at $\langle g \rangle = 1.93$ with

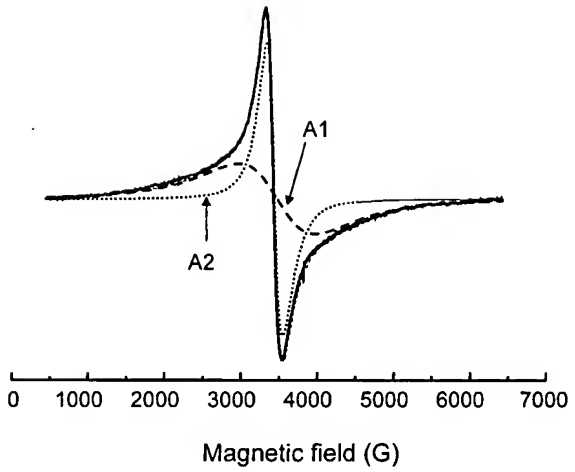

Fig. 3. Deconvolution of the EPR spectrum of sample **MVS** after its use in the catalytic test. The experimental spectrum is shown as a thicker gray line with the computer simulation being overlapped as a thinner black line and the individual signals as dotted black lines.

$\Delta H_{pp} \approx 1000$ G and a minor axial one at $g_{\perp} = 1.96$ and $g_{\parallel} = 1.90$, signal **A2**, which is narrower than the former (average width ≈ 225 G). It must be noted that signal **A1** could present certain anisotropy, difficult to be resolved as a consequence of its considerable width. Parameters of signals **A1** and **A2** are consistent with the presence of Mo^{5+} cations [16,31]; though their large linewidth does not discard the contribution of other possible paramagnetic cations (like V^{4+}), which could participate into magnetically coupled phases. This is particularly true for the major broader signal **A1**, for which a higher uncertainty in its estimated parameters could be inferred from computer simulations. In any case, the significant width of both signals, with the consequent absence of resolution of hyperfine features on them (it must be considered that ca. 25% of the molybdenum—^{95}Mo and ^{97}Mo isotopes—presents nuclear spin $I = 5/2$, while 99.75% of the vanadium presents $I = 7/2$), suggests that the paramagnetic centers are immersed into magnetically active environments (probably subjected to strong spin–spin interactions and of a considerable magnitude for centers giving rise to signal **A1**). In addition, some of the samples show a set of relatively narrow features overlapped on the spectrum of signals **A1** + **A2**, which corresponds to the presence of residual amounts of isolated V^{4+} species. Another signal represented by a feature appearing at $\langle g \rangle = 3.7$ is apparent for some of the samples, particularly **MVSK-2** and **MVSK-4**, although it can be also present in minor amounts for the other samples. This most likely corresponds to the forbidden transition ($\Delta m_s = \pm 2$) of Mo^{5+} ionic pairs in an excited triplet state [32], based on the fact that a certain intensity increase is observed upon recording the spectrum at 298 K. No systematic study of these aspects has been done since they do not appear of relevance in the context of the present work.

Concerning the quantitative aspects, the overall amount of paramagnetic species detected is 158.8, 167.1, and 178.1 μmol g^{-1}, for **MVS**, **MVSK-2**, and **MVSK-4** samples, respectively, which correspond to about 3% of the total amount of Mo. Concerning the relative contributions of signals **A1** and **A2**, the **A1/A2** intensity ratio displays, according to computer simulation results, values of 4.0, 5.0, and 5.3 for samples **MVS**, **MVSK-2**, and **MVSK-4**, respectively.

Binding energies at peak maximum and peak half widths (FWHM) of the V2p3/2, Mo3d5/2, Sb3d3/2, and K2p3/2 core-level lines in the XPS spectra of the **MVS**, **MVSK-2**, and **MVSK-4** samples, as well as the surface metal atomic ratio determined from XPS data, are given in Table 2. For comparative purposes, the XPS results of the MoVSbO sample calcined initially in air at 553 K and then in N_2 at 873 K (sample **MVS-A-N**) are also included. It can be noticed that the Mo/V/Sb surface atomic ratios of the catalysts remains almost the same after the incorporation of potassium and are in close agreement with the bulk composition (Table 1).

The FWHM values of the Mo3d peaks are similar in all samples and can be fitted with two components at BE = 232.7 and 231.7 eV for the Mo3d5/2 peak, which can be assigned to Mo^{6+} and Mo^{5+} species [24,33–35]. Noteworthy, a Mo^{5+}/Mo_{total} atomic ratio of about 0.35 (Mo^{6+}/Mo^{5+} molar ratio close to 2) is determined for samples calcined under N_2. This contrasts with detection of exclusively Mo^{6+} species for **MVS-A-N**, suggesting that a higher overall oxidation degree is achieved in this sample as a consequence of the intermediate calcination treatment under air performed in this sample, in agreement with XRD results.

The V2p3/2 core-level spectra of all samples can be decomposed into two components at BE = 516.3 and 517.4 eV, which can be assigned to V^{4+} and V^{5+}, respectively [24,35]. V^{4+} cations seem to be the main component in undoped and K-doped catalysts, presenting a V^{4+}/V_{total} atomic ratio of 0.84–0.87 (V^{4+}/V^{5+} molar ratio around 5.5) for **MVS** and **MVSK-***n* samples (Table 3). No V^{3+} species have been detected in these catalysts. However, V^{3+} species (BE = 515.5 eV) are observed in sample **MVS-A-N**, which shows V^{4+}/V_{total} and V^{3+}/V_{total} atomic ratios of 0.61 and 0.29. So, a partial reduction of V^{4+} to V^{3+} is apparently produced for this sample.

While the addition of potassium to the MoVSb oxide does not appear to have a strong influence on the surface composition and the nature of V2p or Mo3d XPS spectra, a different behavior is inferred for Sb, according to the Sb3d XPS spectra (Fig. 4). The peak width of the Sb3d3/2 line is sensitively higher in the K-doped samples than in the samples without potassium (1.95 and 1.70 eV, respectively), which could be related to the presence of another species or to differential charging of the samples. Since no broadening has been observed in the peaks from other zones in the spectra of the K-doped samples, contributions from differential charging of the samples can be neglected. We must indicate that the identification of the Sb oxidation state is complicated because the Sb3d5/2 peaks overlap with O1s peaks and the BE separation of Sb^{3+} and Sb^{5+} is relatively small (approximately 0.6 eV). The deconvolution of the Sb3d3/2 line for

Table 2
XPS results of undoped and K-doped Mo–V–Sb–O catalysts

Sample	Binding energies (peak width)								Me^{n+}/Me_{total} atomic ratio		
	Mo3d5/2		V2p3/2			Sbd3/2		K2p3/2	Mo^{5+}/Mo_{total}	V^{4+}/V_{total} (V^{3+}/V_{total})[a]	Sb^{5+}/Sb_{total}
	Mo^{6+}	Mo^{5+}	V^{5+}	V^{4+}	V^{3+}	Sb^{5+}	Sb^{3+}				
MVS	232.7 (1.79)	231.8 (1.77)	517.4 (1.21)	516.3 (1.78)	–	–	539.5 (1.77)	–	0.35	0.87 (0)[a]	0
MVSK-3	232.7 (1.80)	231.7 (1.70)	517.3 (1.28)	516.3 (1.71)	–	540.2 (1.70)	539.4 (1.77)	292.9 (2.25)	0.26	0.84 (0)[a]	0.29
MVSK-4	232.8 (1.70)	231.9 (1.60)	517.4 (1.20)	516.3 (1.74)	–	540.4 (1.60)	539.5 (1.70)	293.1 (1.90)	0.35	0.84 (0)[a]	0.17
MVS-A-N	232.9 (1.80)	–	517.4 (1.20)	516.4 (1.60)	515.5 (1.60)	540.4 (1.69)	539.4 (1.70)	–	0	0.61 (0.29)[a]	0.81

[a] In parenthesis the V^{3+}/V_{total} atomic ratios calculated from the XPS experiments.

Table 3
Catalytic performance of undoped and K-doped MoVSbO mixed metal oxide catalysts in the selective oxidation of propane[a]

Catalyst	Conversion (%)[b]	Selectivity (%)[c]						
		CH_2:$CHCO_2H$	CH_3CO_2H	C_3H_6	CH_2:CHCHO	CH_3COCH_3	CO	CO_2
MVS	19.8	7.6	27.0	6.7	0.1	3.2	19.5	35.8
MVSK-1	14.3	19.8	16.2	11.5	–	4.6	15.3	32.7
MVSK-2	11.9	34.8	10.6	17.7	0.1	4.2	11.6	21.0
MVSK-3	9.5	34.5	8.4	22.2	–	3.5	11.1	20.3
MVSK-4	7.8	28.1	7.9	28.1	–	6.4	10.3	19.2
MVS-A-N	18.0	13.0	18.2	15.1	–	2.3	18.0	33.5

[a] Reaction conditions: Contact time, W/F, of 510 $g_{cat}\,h^{-1}\,mol^{-1}_{C_3H_8}$; reaction temperature: 613 K; $C_3H_8/O_2/H_2O$/He molar ratio of 4/8/30/58.

[b] Propane conversion (%).

[c] Acetaldehyde has also been observed with selectivities lower than 0.3%.

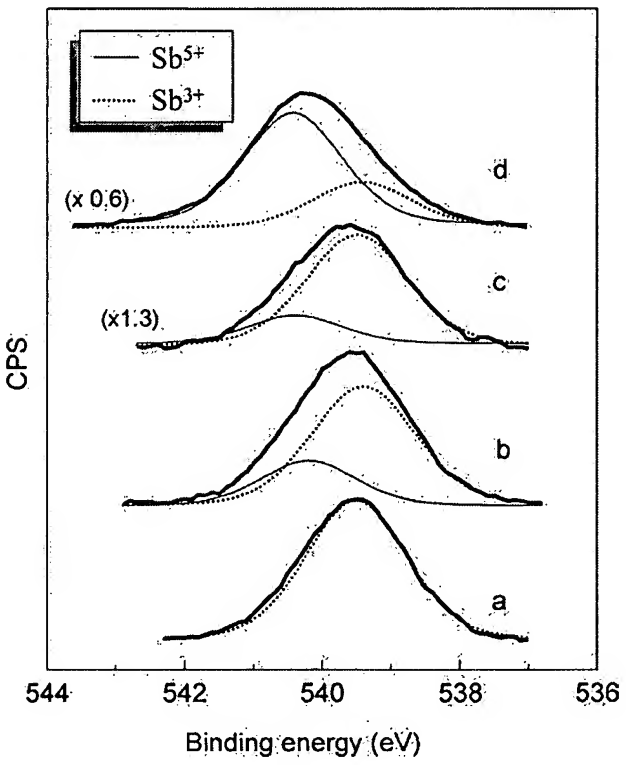

Fig. 4. XPS spectra of Sb3d3/2 in the undoped and K-doped MoVSbO catalysts: (a) MVS; (b) MVSK-2; (c) MVSK-4; (d) MVS-A-N.

the K-doped samples is shown in Fig. 4. The Sb3d3/2 peak of the K-containing samples can be fitted with two components at BE = 540.2 and 539.4 eV, assigned to Sb^{5+} and Sb^{3+}, respectively [26,36,37], while only one component at BE = 539.5 eV, of Sb^{3+}, is observed in the K-free sample.

These results suggest an oxidation of Sb^{3+} to Sb^{5+} on the catalyst surface (with Sb^{5+}/Sb_{total} atomic ratios of 0.17–0.29) after the incorporation of potassium. However, the formation of Sb^{5+} species is lower than that observed in the sample **MVS-A-N** (Sb^{5+}/Sb_{total} atomic ratios of 0.81). Such on-surface oxidation is not a consequence of the presence of oxygen during the calcination of these samples, but it could be related with the presence of nitrates (from the KNO_3 used to incorporate potassium) during the calcinations step. In fact, when the MoVSb precursor is calcined initially with O_2 and then with N_2 (sample **MVS-A-N**), the partial oxidation of Sb^{3+} to Sb^{5+} is accompanied by partial reduction of V^{5+} to V^{4+} and V^{3+}, although without apparent modification of the oxidation state of Mo (Mo^{6+}). At this point, it has to be said that in V–Sb-containing catalysts Sb^{5+} species are formed from Sb^{3+} at the expense of the partial reduction of V^{5+} to V^{4+} and V^{3+} [36,37], although, in the presence of Mo^{6+}, V^{3+} formed is rapidly oxidized to V^{4+} with the formation of Mo^{5+}.

Fig. 5 shows the normalized XANES region of the absorption spectra at the Sb L_I edge of samples **MVS**, **MVSK-3**, and **MVS-A-N** and those of $FeSbO_4$ and Sb_2O_3 used as

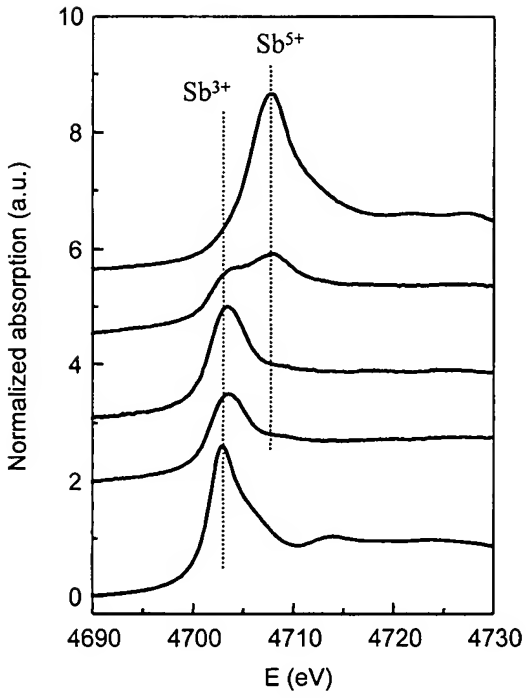

Fig. 5. Normalized XANES spectra at the Sb L_I edge of samples: (a) Sb_2O_3, (b) **MVS**, (c) **MVSK-3**, (d) **MVS-A-N**, and (e) $FeSbO_4$.

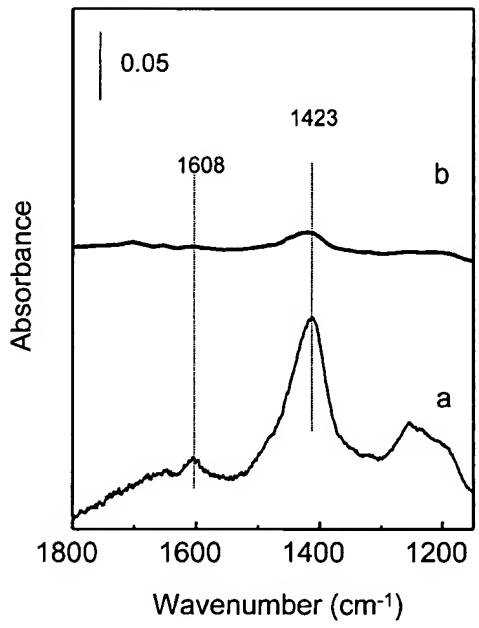

Fig. 6. FTIR spectra of NH_3 adsorbed on undoped and K-doped samples after evacuation at 373 K: (a) **MVS**; (b) **MVSK-3**.

references. The edge maximum corresponds to the electronic transition from the $2s_{1/2}$ to the empty 5p orbital, and the energy involved strongly depends on the occupancy of the 5s orbital, i.e., on the presence of Sb^{3+} or Sb^{5+}. The edge position is very sensitive to the oxidation state of antimony, appearing at 4703.0 eV for Sb^{3+} and at 4708.0 eV for Sb^{5+}, as can be observed for Sb_2O_3 and $FeSbO_4$, respectively, in Fig. 5. This renders XANES spectroscopy very valuable for determining the valence of antimony, information which is not easily available by any other technique.

The spectra of the K-free and K-containing **MVS** samples (see Fig. 5, spectra b and c) exhibit the edge maxima at 4703.4 eV, clearly indicating that antimony is present as Sb^{3+} in both oxides [26]. However, when the parent **MVS** oxide is calcined in air before the treatment in N_2, i.e., sample **MVS-A-N**, the maximum is shifted at 4708.0 eV characteristic of Sb^{5+}, while a shoulder at ca. 4703 eV of Sb^{3+} is also observed, evidencing the presence of antimony in both oxidation states (Fig. 5d). Fitting the spectrum using a combination of the two references for Sb^{3+} and Sb^{5+} the Sb^{3+}/Sb^{5+} ratio can be estimated to be approximately 1. Therefore, bulk oxidation of Sb^{3+} occurs upon the calcination in air of a MoVSbO sample (**MVS-A-N**) but not upon incorporation of potassium.

Reported in Fig. 6 are the infrared spectra of ammonia adsorbed on undoped (Fig. 6a) and K-doped (Fig. 6b) MoVSbO catalysts after evacuation at 373 K. The adsorption band at 1608 cm^{-1} can be attributed to the asymmetric bending vibration of ammonia adsorbed on Lewis acid sites, while the band at 1423 cm^{-1} corresponds to an asymmetric deformation vibration (δ_{as}) of the ammonium ions (NH_4^+) on Brønsted acid sites [38]. The broadening of the latter band must be related to a certain heterogeneity in the Brønsted acid sites, or to a splitting of the δ_{as} vibration as a consequence of changes in the adsorption symmetry of the NH_4^+ molecule at the catalyst surface.

The incorporation of potassium apparently decreases the intensity of both bands, thus confirming the diminution of the number of acid sites of the catalyst as already observed upon incorporation of alkali metals on V- or Mo-based catalysts [39–43].

Conversely, no significant structural changes have been detected by XRD in the **MVS** and K-doped catalysts after the catalytic test, and only the **MVA-A-N** sample shows a slight decrease in the intensity of the peaks corresponding to MoO_3 (Fig. 1d). The XPS study of the undoped and K-doped MoVSbO used samples shows neither changes in the catalyst composition nor important variations in the oxidation state of each element on the catalyst surface. In addition, Sb^{3+} was also mainly observed by EXAFS in the used catalysts. Therefore, we can assume that, under the reaction conditions used in this work, our catalysts are reasonably stable during the reaction tests.

3.2. *Catalytic results for the selective oxidation of propane*

Fig. 7 reports the variation of the propane conversion and the selectivities to the main reaction products obtained during the oxidation of propane in the 613–673 K temperature range, while Table 3 summarizes the catalytic results obtained during the oxidation of propane at 653 K on undoped and K-doped catalysts. Partial oxidation products (propylene, acrylic acid, acrolein, acetone, and acetic acid) and

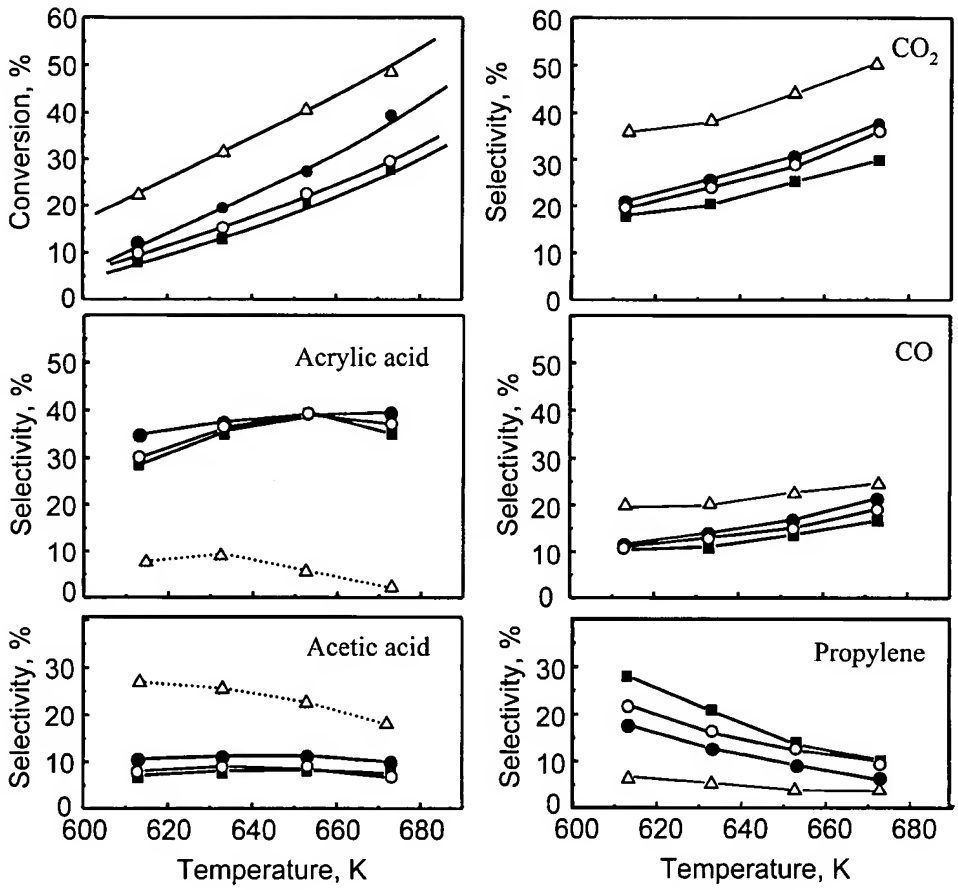

Fig. 7. Variation of the propane conversion and the selectivities to the main reaction products with the reaction temperature obtained during the oxidation of propane at 653 K over the undoped and K-doped catalysts: MVS (△); MVSK-2 (●); MVSK-3 (○); MVSK-4 (■). Contact time, W/F, of 510 $g_{cat}\,h^{-1}\,mol_{C3}^{-1}$.

carbon oxides have been observed in all cases, although their corresponding selectivities strongly depend on the catalyst composition.

The undoped **MVS** sample presents a very low selectivity to acrylic acid but an important selectivity to acetic acid. Comparing the samples **MVS** and **MVS-A-N**, it can be concluded that no apparent modification in the catalytic performance occurs when the sample is previously calcined in air at 553 K before the heat treatment at 873 K in N_2 (Table 3).

The catalytic behavior of MoVSbO catalysts is completely modified when potassium is added to the catalyst (Fig. 7 and Table 3). The incorporation of small amounts of potassium notably increases the selectivity to acrylic acid and propylene, decreasing the selectivity of both acetic acid and carbon oxides. However, the propane conversion decreases with increasing the K content in the catalyst. In this way the sample with a K/Mo ratio of 0.02 presents less than half of propane conversion than the undoped samples.

A relative increase in the selectivity to organic acids (acrylic and acetic acids) without apparent changes in the propane conversion has been obtained when a MoVSbO catalyst was treated with a K-free aqueous solution following a procedure similar to that used for the preparation of the K-containing samples [27] or by grinding a $Mo_6V_2SbO_x$ catalyst [23]. However, the increase in the selectivity to acrylic acid in the last two cases was very modest compared to the changes obtained for the K-doped catalysts. So, the changes observed in the K-doped catalysts cannot be explained by mechanical modifications of the crystalline phases, but by the effect of K-induced modification of the catalyst surface.

The results of Fig. 7 indicate that the selectivity to propylene decreases and the selectivity to acrylic acid increases when the reaction temperature increases. However, the effect of the reaction temperature on the selectivity to acrylic acid is a consequence of the variation of the propane conversion. In this way, the highest selectivity to acrylic acid was observed at propane conversions between 20 and 30%.

The yields of partial oxidation products, i.e., acrylic acid, propylene, and acetic acid, obtained at 653 K over the studied catalysts are reported in Fig. 8. An opposite trend in the yields of acetic and acrylic acids is observed when the amount of potassium incorporated to the catalysts is increased, whereas the yield of propylene remains almost unchanged. Moreover, no changes in the sum of the yield of partial oxidation products (acrylic acid, acetic acid, and propylene) are apparently observed when the amount of potassium on the catalysts is changed. Therefore, the

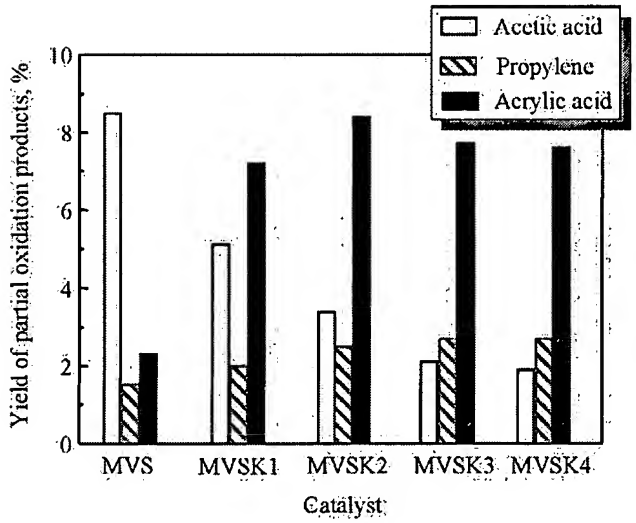

Fig. 8. Yield of acetic acid, propylene, and acrylic acid obtained during the oxidation of propane at 653 K over undoped and K-doped samples. Contact time, W/F, of 510 $g_{cat}\,h^{-1}\,mol^{-1}_{C3}$.

lower conversion observed in the K-doped catalysts must be mainly related to a decrease in the formation of carbon oxides. So, the incorporation of potassium favors an enhancement of both the selectivity and the yield of acrylic acid by decreasing the formation of both acetic acid and carbon oxides. It must be noted that the yields to acrylic acid obtained over the K-doped samples are higher than those previously reported in the literature for MoVSbO [23] or Nb-containing MoVSbO catalysts [20–22], although lower than those reported in the patent literature [19,44].

In order to gain a better understanding of the different pathways in the mechanism for propane oxidation, we have carried out some experiments of propylene oxidation, since propylene can be considered as intermediate in propane oxidation. Table 4 shows the catalytic results obtained during the propylene oxidation on undoped and K-doped catalysts. Acrylic acid, acetic acid, acetone, and carbon oxides are mainly observed, while acrolein and acetaldehyde were detected with very low selectivities. Acetone was the most important partial oxidation reaction product at low temperatures and low propylene conversions, while acrylic acid (mainly obtained on K-doped catalysts) and/or acetic acid (mainly obtained on undoped **MVS** samples) were obtained at high reaction temperatures and high propane conversions. This trend is similar to that observed during the propane oxidation.

4. Discussion

4.1. On the catalyst characterization

The characterization results presented here suggest that the incorporation of K modifies only the characteristics of the surface of the MoVSbO catalyst, although whether changes in the nature of the crystalline phases are induced is still unclear. The XRD patterns of K-free and K-doped catalysts suggest the presence of similar crystalline phases. According to this, SEM/EDX results indicate the presence of essentially two compositionally different zones in the catalysts. Vanadium appears homogeneously distributed in the crystallites, which suggests that it is incorporated to the structure of Mo–Sb–O mixed oxide, as already proposed for Mo–V–Te–Nb–O [24] and Mo–V–Sb–O mixed oxides [23]. However, the XRD by itself cannot be used in the determination of the crystalline phases in these catalysts. In fact, recent results published on MoVSbO [23] and MoVSbNbO [20,21] catalysts suggest the presence of several SbMoVO crystalline phases depending on the calcination conditions: $Sb_4Mo_{10}O_{30}$ and $Sb_2Mo_{10}O_{31}$ in samples heat-treated at 873 K in N_2 and activated in He [20,21] and $(Sb_2O)M_6O_{18}$ and $(SbO)_2M_{20}O_{56}$ (with M = Mo and V) in samples activated in air at 643 K for 20 min followed by a second heat treatment, in pure nitrogen, at 873 K for 2 h [26]. Moreover, the XRD pattern of $Sb_4Mo_{10}O_{30}$ is similar to that shown by $(Sb_2O)M_6O_{18}$, while the XRD pattern of $Sb_2Mo_{10}O_{31}$ is similar to that of $(SbO)_2M_{20}O_{56}$, making difficult an un-

Table 4
Catalytic performance of undoped and K-doped MoVSbO mixed metal oxide catalysts in the selective oxidation of propylene[a]

Catalyst	Temperature (K)	Conversion (%)[b]	Selectivity (%)[c]					
			CH_2:$CHCO_2H$	CH_3CO_2H	CH_2:CHCHO	CH_3COCH_3	CO	CO_2
MVS	593	42.9	27.0	8.4	0.2	35.3	14.5	14.4
	613	56.3	32.0	12.4	0.1	14.7	21.5	19.2
	638	68.4	21.0	13.0	0.1	6.0	36.0	33.4
MVSK-2	614	29.1	36.6	6.3	0.3	31.6	13.2	12.0
	636	39.1	46.4	7.7	0.2	14.3	17.0	14.3
	653	50.6	46.0	7.5	0.1	5.8	22.2	18.4
MVSK-4	613	19.0	36.0	3.0	0.5	42.0	10.2	8.3
	634	27.8	51.1	4.8	0.4	19.7	13.7	10.3
	654	34.9	59.6	4.1	0.3	7.7	16.1	12.1

[a] Reaction conditions: $C_3H_6/O_2/H_2O$/He molar ratio of 4/9/30/57 and contact time, W/F, of 100 $g_{cat}\,h^{-1}\,mol^{-1}_{C_3H_6}$.

[b] Propylene conversion (%).

[c] Acetaldehyde was also observed with a selectivity lower than 0.3%.

ambiguous attribution of the diffraction peaks. The most important differences among these crystalline phases appear to be related to the oxidation states of Sb: only Sb^{3+} is present in $Sb_4Mo_{10}O_{30}$ and $Sb_2Mo_{10}O_{31}$ [20,25], while Sb^{3+} and Sb^{5+} are observed in $(Sb_2O)M_6O_{18}$ (with a Sb^{3+}/Sb^{5+} ratio of 63/37) and $(SbO)_2M_{20}O_{56}$ (with a Sb^{3+}/Sb^{5+} ratio of 11/89) [26]. So, a possible discrimination between these structures could be established on the basis of the presence of Sb ions with different oxidation states.

Therefore, the presence of both Sb^{3+} and Sb^{5+} in **MVS-A-N**, determined by XANES, suggests the possible presence of $(Sb_2O)M_6O_{18}$ and $(SbO)_2M_{20}O_{56}$ (with M = Mo and V), rather than $Sb_4Mo_{10}O_{31}$ and $Sb_2Mo_{10}O_{31}$ [26], in catalysts first calcined in oxygen and then heat-treated in N_2. Sb^{5+} species have not been observed by XANES in both undoped and K-doped catalysts heat-treated in N_2, i.e., **MVS** and **MVSK-n** series, suggesting the presence of $Sb_4M_{10}O_{31}$ and $Sb_2M_{10}O_{31}$ (with M = Mo and V). Only a partial oxidation of surface Sb^{3+} to Sb^{5+} species, which are not observed in the undoped sample, and a decrease in the number of acid sites, especially of Brønsted type, are observed upon the addition of potassium on the surface of the MoVSbO mixed oxide.

The EPR experiments evidence the presence of two different magnetic environments for the paramagnetic cations (Mo^{5+} and possibly also V^{4+}), corresponding to signals **A1** and **A2**. It is tempting to establish a correlation between the two signals and the presence of two distinct phases (as suggested also by the EDX results of Table 1) into which the corresponding paramagnetic species would be immersed. The larger width of signal **A1** suggests shorter average distances between the spins, and then a higher concentration of Mo^{5+} (and V^{4+}) species would be expected in this magnetic domain. It must be noted that the amount of paramagnetic species detected in these spectra is relatively low when compared to the total amount of Mo and V (around 3%, considering the sample compositions determined by AAS, Table 1). The considerable higher concentration of paramagnetic species obtained by XPS (Table 2) and the low surface area of these oxides (Table 1) would suggest that they are exclusively located at surface or near surface. However, this is not consistent with the presence of mixed valence (Mo^{6+}/Mo^{5+} or V^{5+}/V^{4+}) phases observed by XRD. In fact, the EPR spectrum of sample **MVS** recorded under air (at atmospheric pressure) shows almost no modification in the signals lineshape or amplitude, suggesting a bulk nature for most of the detected paramagnetic centers. Therefore, it appears that a significant amount of the paramagnetic species must escape detection due to antiferromagnetic couplings [45].

Moreover, the relatively low amount of Sb^{5+} species detected by XPS on the surface of K-doped catalysts and the fact that Sb^{5+} species are not detected by XANES, along with consideration that structural or chemical transformations induced by K ions must mainly affect the catalyst surface, suggest that oxidized Sb^{5+} is only located on the catalyst surface. A different conclusion can be proposed in the sample initially calcined in air and then heat-treated in N_2 (sample **MVS-A-N**). The XPS spectra of this sample suggest a high Sb^{5+}/Sb^{3+} ratio on the surface, besides several oxidation states for V, i.e., V^{5+}, V^{4+}, and V^{3+}, with a higher overall reduction state. These results suggest that a different solid-state reaction occurs upon calcination of the sample under oxygen, which favors a redox reaction between V and Sb, as suggested in other V–Sb–O-based catalysts [35,36].

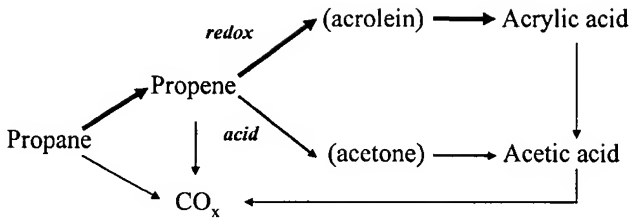

Scheme 1. Reaction network for the oxidation of propane on MoVSb-based catalysts.

4.2. Selective oxidation of propane on undoped and K-doped MoVSbO catalysts

According to our results, a reaction network of propane oxidation similar to that previously reported for MoVTe- [16,24,46,47] or MoVSb-based [20–23] catalysts can be proposed (Scheme 1), with a higher selectivity to acetone and acetic acid over the latter. Propylene is initially formed from propane on both undoped and K-doped catalysts. According to the results of Table 4, propylene can consecutively react on the catalyst surface giving three parallel reactions: (i) partial oxidation to acrolein/acrylic acid; (ii) hydration and oxidative scission to acetone/acetic acid; (iii) direct oxidation to carbon oxides. It is clear that the modification of the catalyst surface by the K incorporation strongly changes the reaction rates of the parallel reactions. In this way, a higher formation of acrylic acid and a lower formation of acetic acid and carbon oxides have been observed in the K-doped catalysts (Fig. 7).

It is generally accepted that both the selective oxidation and the oxidative dehydrogenation of propane are initiated via H abstraction from propane by a concerted mechanism over acid–base pairs [3,4,16–18,21–24]. The Lewis acid site (V^{5+} cation) and basic oxygen (O^{2-}) interacts with the α- and β-hydrogen of propane, respectively, to form propylene [24,48]. The incorporation of K ions on the surface of V- [39–41] or Mo-based [41–43] catalysts has been reported to modify the acid character and the nature of surface metal species, favoring the achievement of higher selectivities to propylene from propane. Accordingly, the incorporation of potassium to MoVSbO catalysts is expected to increase the selectivity to propylene during the oxidative dehydrogenation [39–43], but it is apparently surprising the fact that the selectivity to acrylic acid is also increased.

It is known that acid sites favor the formation of acetic acid, and that V_2O_5–MoO_3 catalyst favors the oxidative scis-

sion of propylene in the presence of water vapor to form acetone/acetic acid [49]. Meanwhile, alkaline cations promote the allylic oxidation of propylene or butylenes over Mo-containing catalysts [50,51]. According to these results, the incorporation of potassium to the MoVSbO catalyst surface decreases the number of acid sites, and then the formation of both acetic acid and carbon oxides. A similar effect is observed upon the addition of H_2O in the feed, which enhances the selectivity to acrylic acid during the oxidation of propane on MoVSbNbO [22] or VPO [6]. So, it appears that the elimination of the strongest acid sites favors the partial oxidation rather than the hydration (and the oxidative scission) reaction.

Beside the decrease in the surface acidity, the incorporation of K on the surface of the MoVSbO catalyst provokes the partial oxidation of surface Sb^{3+} to Sb^{5+}, which could favor the formation of acrylic acid by an allylic mechanism [18]. However, the catalytic results over **MVS** (Sb^{3+}) and **MVS-A-N** (Sb^{3+}/Sb^{5+}) suggest no apparent influence of the oxidation state of Sb on catalytic behavior, and then that the increase in the selectivity to acrylic acid on K-doped MoVSbO catalysts must be mainly due to changes in the catalyst acidity.

At the moment, it is not possible to establish the position of K^+ cations at the catalyst surface. Potassium could be located over oxygen atoms of Mo, V, or Sb, replacing surface protons and giving rise to Me–O–K surface bonds, or into the empty channels of the crystalline phases. Though the K^+ cations seems to favor, directly or indirectly, the appearance of Sb^{5+} species on the catalyst surface, the mechanism is still unclear. A higher effort will be made in order to clarify the nature of active sites in each reaction step (oxidative dehydrogenation, O insertion or oxidative scission) as well as the sites in which potassium cations are incorporated.

5. Conclusions

In conclusion, the incorporation of potassium on the surface of MVSbO catalysts enhances the formation and the selectivity to acrylic acid and decreases the formation of acetic acid and carbon oxides during the oxidation of propane. The presence of potassium diminishes the acidity of the catalyst surface, avoiding undesiderable reactions and favoring the selective formation of acrylic acid.

No important modification in the characteristics of the catalysts has been observed after the incorporation of potassium. In fact, the main characterization results (XRD, SEM, EDX, FTIR, EPR, and XANES) suggest clearly that $Sb_4M_{10}O_{30}$ and $Sb_2M_{10}O_{31}$ (with Sb^{3+} and M = Mo and V) are mainly present in undoped and K-doped catalysts heat-treated in N_2, whereas $(Sb_2O)M_6O_{18}$ and $(SbO)_2M_{20}O_{56}$ (with Sb^{3+}/Sb^{5+} and M = Mo and V) can be proposed as major phases in the sample first calcined in air and then heat-treated in N_2. Moreover, a partial oxidation of Sb^{3+} to Sb^{5+} (Sb^{5+}/Sb_{total} of 0.2–0.3) is observed on the surface of the K-doped catalysts, probably as a consequence of the presence of nitrates during the calcination of doped samples.

A further "in-situ" study of these catalysts will help to determine the exact nature of crystalline phases and the possible incorporation of V species in the structure of Mo–Sb–O mixed oxides.

Acknowledgments

This work was carried out under the financial support of the Spanish CICYT (Project PPQ2003/03946). Thanks are due to Dr. A. Mifsud for her discussion in SEM/EDX results and Prof. J. Soria for the use of the EPR spectrometer. The authors thank LURE for technical assistance and by the inclusion in the European Training and Mobility Program, special thanks are given to Dr. A. Traverse.

References

[1] R.E. Kirk, F. Orthmer, J.I. Kroschwitz, M. Howe-Grant, Kirk-Othmer's Enciclopedia of Chemical Technology, Wiley, New York, 1991.
[2] N. Nojiri, Y. Sakai, Y. Watanabe, Catal. Rev. Sci. Eng. 37 (1995) 145.
[3] T. Ushikubo, Catal. Today 78 (2003) 43.
[4] M.M. Lin, Appl. Catal. A 207 (2001) 1.
[5] M. Ai, Catal. Today 42 (1988) 297.
[6] G. Landi, L. Lisi, J.C. Volta, Chem. Commun. (2003) 492.
[7] Y.-F. Han, H.-M. Cheng, H. Wang, J.F. Deng, Chem. Commun. (1999) 521.
[8] A.C. Kaddouri, C. Mazzocchia, E. Tempesti, Appl. Catal. A 180 (1999) 271.
[9] N. Fujikawa, K. Wakui, K. Tomita, W. Onoe, W. Ueda, Catal. Today 71 (2001) 83.
[10] N. Mizuno, M. Tateishi, M. Iwamoto, Appl. Catal. A 128 (1995) L165.
[11] H.-S. Jiang, X. Mao, S.-J. Xie, B.-K. Zhong, J. Mol. Catal. A 185 (2002) 143.
[12] W. Li, K. Oshihara, W. Ueda, Appl. Catal. A 182 (1999) 357.
[13] J.H. Holles, C.J. Dillon, J.A. Labinger, M.E. Davis, J. Catal. 218 (2003) 42.
[14] M.E. Davis, C.J. Dillon, J.H. Hollesand, J.A. Labinger, Angew. Chem. Int. Ed. 41 (2002) 858.
[15] T. Ushikubo, N. Hiroya, K. Yukio, W. Shin, US patent 5,380,993 (1995).
[16] P. Botella, J.M. López Nieto, B. Solsona, A. Martinez-Arias, Catal. Lett. 74 (2001) 149.
[17] H. Tsuji, Y. Koyasu, J. Am. Chem. Soc. 124 (2002) 5608.
[18] R.K. Grasselli, J.D. Burrington, D.J. Buttrey, P. DeSanto, C.G. Lugmair, A.F. Volpe, T. Weingand, Top. Catal. 23 (2003) 5.
[19] H. Hinago, K. Hiroyuki, DE patent 10,145,958 A1 (2001).
[20] J.C. Vedrine, E.M. Novakova, E.G. Derouane, Catal. Today 81 (2003) 27.
[21] E.M. Novakova, J.C. Vedrine, E.G. Derouane, J. Catal. 211 (2002) 235.
[22] E.M. Novakova, E.G. Derouane, J.C. Vedrine, Catal. Lett. 83 (2002) 177.
[23] W. Ueda, K. Oshihara, Appl. Catal. A 200 (2000) 135.
[24] P. Botella, J.M. López Nieto, B. Solsona, A. Mifsud, F. Márquez, J. Catal. 209 (2002) 445.
[25] M. Parmentier, C. Gleitzer, R.J.D. Tilley, J. Solid State Chem. 31 (1980) 305.
[26] J.M.M. Millet, M. Baca, A. Pigamo, D. Vitry, W. Ueda, J.L. Dubois, Appl. Catal. A 244 (2003) 359.

[27] P. Botella, P. Concepción, J.M. López Nieto, B. Solsona, Catal. Lett. 89 (2003) 249.
[28] C.D. Wagner, L.E. Davis, M.V. Zeller, T.A. Taylor, R.H. Raymond, L.H. Gale, Surf. Interface Anal. 3 (1981) 211.
[29] M. Wark, M. Koch, A. Bückner, W. Grünert, J. Chem. Soc., Faraday Trans. 94 (1998) 2033.
[30] J.C.J. Bart, F. Cariati, A. Sgamelloti, Inorg. Chim. Acta 36 (1979) 105.
[31] K. Dyrek, M. Che, Chem. Rev. 97 (1997) 305.
[32] E. Abi-Aad, A. Bennani, J.-P. Bonnelle, A. Aboukais, J. Chem. Soc., Faraday Trans. 91 (1995) 99.
[33] K. Asakura, K. Nakatani, T. Kubota, Y. Iwasawa, J. Catal. 194 (2000) 309.
[34] J.M.M. Millet, H. Roussel, A. Pigamo, J.L. Dubois, J.C. Jumas, Appl. Catal. A 232 (2002) 77.
[35] V. Bondarenka, S. Grebinskij, S. Kaciulis, G. Mattogno, S. Mickevicius, J. Electron Spectrosc. Relat. Phenom. 107 (2000) 253.
[36] J. Nilson, A.R. Landa-Cánovas, S. Hansen, A. Andersson, J. Catal. 186 (1999) 442.
[37] A. Andersson, S.L.T. Andersson, G. Centi, R.K. Grasselli, M. Sanati, F. Trifiró, Appl. Catal. A 113 (1994) 43.
[38] H. Knözinger, in: G. Ertl, H. Knözinger, J. Weitkamp (Eds.), Handbook of Heterogeneous Catalysis, vol. 2, VCH, New York, 1997, p. 707.
[39] J.M. López Nieto, R. Coenrads, A. Dejoz, M.I. Vázquez, Stud. Surf. Sci. Catal. 110 (1997) 767.
[40] T. Blasco, J.M. López Nieto, Appl. Catal. A 157 (1997) 117.
[41] B. Grzybowska-Swierkosz, Top. Catal. 21 (2002) 35.
[42] R.B. Watson, U.S. Ozkan, J. Catal. 191 (2000) 12.
[43] K. Chen, S. Xie, A.T. Bell, E. Iglesia, J. Catal. 195 (2000) 244.
[44] M. Takahashi, X. Tu, T. Hirose, M. Ishii, US patent 5,994,580 (1999).
[45] L. David, C. Craciun, M. Rusu, D. Rusu, O. Cozar, J. Chem. Soc., Dalton Trans. (2000) 4374.
[46] L. Luo, J.A. Labinger, M.E. Davis, J. Catal. 200 (2001) 222.
[47] M. Lin, T.B. Desai, F.W. Kaiser, P.D. Klugherz, Catal. Today 61 (2000) 223.
[48] T. Shishido, T. Konishi, I. Matsuura, Y. Wang, K. Takaki, K. Takehira, Catal. Today 71 (2001) 77.
[49] T. Seiyama, K. Nita, T. Mahehara, N. Yamazoe, Y. Takita, J. Catal. 49 (1977) 164.
[50] C. Martin, I. Martin, C. Mendizábal, V. Rives, Stud. Surf. Sci. Catal. 75 (1993) 1987.
[51] P. Forzatti, F. Trifiró, P.L. Villa, J. Catal. 52 (1978) 389.